Vol. 10. Issue 1, 2024

ISSN: 2453-7314

Central European Researchers Journal

CERES

A Word of Welcome from the Editors

Dear Colleagues, Readers and Authors,

We are pleased to present the latest issue of our journal, dedicated to the newest trends, research, and achievements in the field of technical cybernetics. In this edition, we bring you a selection of articles that reflect the progress and innovative projects within this dynamically evolving domain.

Among the topics, you will find Solar Charging Control System, Modernization of the Transport Laboratory, and Solar Car: Example of Low Power Design. Additionally, the issue includes studies on Intelligent Power Sockets and Energy Storage Systems - a Way of Increasing Operational Time of WSN Devices.

Students have actively collaborated on several projects, highlighting their crucial role in research and development. Their contributions are particularly evident in projects such as Automated Terrarium Implementation and ESP32-Based Pulse Oximeter Design. These experiences not only advanced specific technologies but also provided students with valuable practical knowledge.

The vision of this journal is to deliver information that is both valuable and beneficial to everyone interested in advancements in cybernetics. We wish you an enjoyable reading experience and many inspiring insights!

Sincerely,

The Editorial Team

Central European Researchers Journal. Volume 10. Issue 1
Editor-in-chief: Kharchenko Vyacheslav, Zaitseva Elena

Addres of the editorial office: Central European Researchers Journal - editorial, Faculty of Management Science and Informatics, University of Zilina, Univerzinta 8215/1, 01026, Zilina, Slovakia, editorial@ceres-journal.eu
Each paper was reviewed by reviewers.
Publisher: JMTM, s.r.o., Sad SNP 8, 010 01, Zilina, Slovakia, publisher@jmtm.sk
Published biannually
ISSN: 2453-7314
July 2024

Contents

Solar Charging Control System

Peter Kolok, Peter Ševčík

Abstract— The result of the work is the creation of an energy-efficient device based on the WIO RP2040 module from the Seeed Studio company, which can effectively search for the angle under which the highest measured intensity of solar radiation is found and then ensure positioning to this angle. By achieving such a state, we can charge the Li-ion battery, which also powers this device. It was necessary to achieve the smallest possible losses and therefore it was important to save energy wherever possible, for the best possible result.

Keywords— Wio, RP2040, Li-ion

I. INTRODUCTION

Solar energy harnessed from the sun can be utilized almost anywhere sunlight reaches the Earth's surface. Solar panels, made up of numerous solar cells, offer an efficient method for converting sunlight into electricity. These panels are employed across various levels, including the commercial sector, in mini-grid systems, and for individual use. They have proven to be an ideal energy source for powering mini-grids, particularly in areas lacking access to mains electricity. This is especially crucial for developing countries that have a high potential for solar radiation.

A. Advantages of Solar Charging

Solar charging offers several significant advantages that contribute to its growing relevance and popularity. First, solar energy is a renewable resource available in any location that receives sufficient sunlight. Additionally, it is environmentally friendly; using solar panels does not contribute to pollution and helps reduce the overall carbon footprint. While the initial investment in solar panels may be higher, they prove to be economically beneficial in the long term because they do not require a continuous supply of fuel.

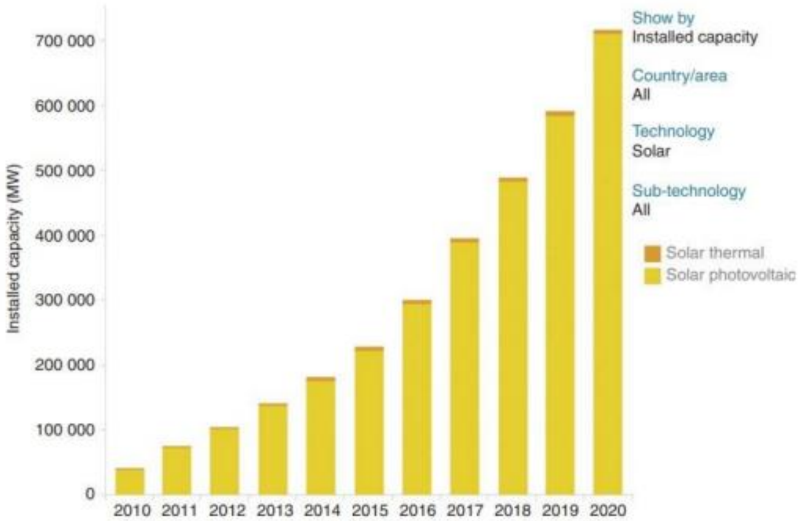

Figure 1 *Increase in solar panel installation over time*

Furthermore, the increasing availability and decreasing solar technology costs support these advantages.

Peter Kolok, University of Žilina, Slovak Republic (e-mail: kolok@stud.uniza.sk)
Peter Ševčík, University of Žilina, Slovak Republic (e-mail: peter.sevcik@fri.uniza.sk)

B. Applications of Solar Charging in Practice

Solar charging is widely used in areas without reliable access to electricity, such as remote regions, developing countries, and rural areas. It powers portable devices like mobile phones, tablets, and GPS units, and serves as a backup energy source for home battery systems, ensuring operation during power outages.

C. Enhancing Energy Harvesting Efficiency

Optimal positioning of solar panels enhances energy generation by ensuring consistent alignment with the sun. A dual-motor system can adjust the panel's angle and orientation for effective energy harvesting. To conserve energy, repositioning can be programmed at intervals, such as every three hours. Fast and precise adjustments further improve efficiency by minimizing energy consumption during realignment.

II. CONTROL SYSTEM SOLUTION

To enhance charging efficiency by repositioning devices, choosing suitable components and creating an effective algorithm for managing their placement is vital.

A. Selection of suitable components

Initially, the ESP32 processor was considered for this project due to its wide range of capabilities. However, the RP2040 was ultimately selected for its high energy efficiency in low-power modes. To enhance power management, the Wio RP2040 module, which features the RP2040 processor, was chosen.

The project also includes components such as a solar cell, two servomotors, step-up modules, a charging module, and a Li-ion battery. A solar cell measuring 70x90 mm, capable of generating 5V and 160mA, was more than sufficient for our needs. For the servomotors, we used a 180-degree (SG90) motor and a 360-degree (DS04-NFC) motor. The device is powered by a standard rechargeable Li-ion battery with a voltage of 3.7V and a capacity of 2500 mAh.

To drive the servomotors, we employed a step-up module (SX1308) to efficiently convert the battery voltage to 5V at 2A, ensuring adequate power for both motors. For efficient charging, we selected the TP4056 charging module, specifically designed for charging Li-ion batteries.

B. Selection of suitable algorithm

To create an effective algorithm, it is essential first to establish a clear objective. In this case, the objective is to charge the Li-ion battery as efficiently as possible by optimizing the positioning of the solar cell. The positioning should be adjusted at regular intervals, such as every hour, to maintain optimal energy collection. Additionally, it would be practical to monitor the battery voltage levels, providing the user with insight into the charging status. It is also important to consider possible events, such as an unknown object obstructing the sunlight reaching the solar cell. For simplicity of implementation, the MicroPython programming language was selected.

C. Implementation of the device

After selecting the components, a printed circuit board (PCB) was designed, on which all the components were assembled. The design of the PCB and the interconnection of the components were based on the structure of the block diagram.

According to the block diagram, the device was designed to include a mechanical switch. This switch allows the user to choose between charging the battery directly from the solar cell or, if the device is connected to a computer (or another peripheral), charging from that source. The device also features three buttons: the first button restarts the search for the highest radiation intensity, the second button serves as a RESET, and the third button is used for BOOT.

An RGB LED was added to indicate errors or to display the device's status.

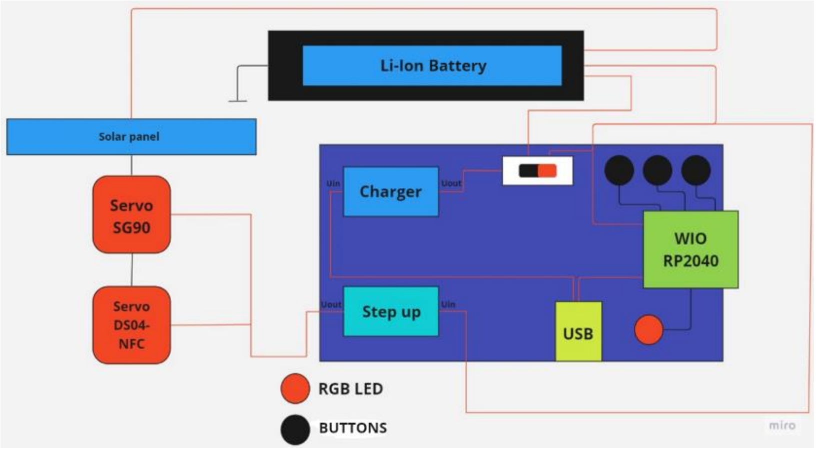

Figure 2 Device block diagram

III. Use in practice

The device must work with efficiency, energy management, and precise placement to increase the efficiency of solar charging.

A. Principle of operation of the device

At the beginning, when the button is pressed, the device initializes, setting the upper servo motor (SG90) to a 40-degree angle. Subsequently, the lower servo motor (plate_number_1) begins to rotate the structure through 360 degrees. During this rotation, the voltage of the solar cell is measured using a voltage divider. Once the scanning process is complete, the device adjusts its position to the angle that recorded the highest light intensity. After this adjustment, the upper servo motor (SG90) activates again to reposition the solar cell, aiming to achieve maximum light intensity.

B. Signaling and Sleep Mode

After identifying the optimal position, the RGB LED indicates the system's status. If the solar cell generates enough voltage to charge the battery, the green LED will flash. If the voltage is insufficient, the red LED will flash instead. Following the green LED signal, the blue LED blinks 20 milliseconds later to indicate that the charging process has begun. Once the charging is complete, the Wio RP2040 enters sleep mode to conserve energy.

C. Periodic Repositioning Using RTC Timers

The device uses a Real-Time Clock (RTC) timer to wake up every hour and automatically adjust its position to the angle with the highest light intensity. In addition, a secondary RTC timer activates the device every 10 minutes for a duration of 1 millisecond to check if any object, such as a cloud, is obstructing the solar cell.

If shading is detected, the device will attempt to reposition itself to find a new optimal angle. If it is unable to achieve sufficient light intensity to charge the battery, it will revert to its previous position and stop further attempts to reposition. However, the 10-minute RTC timer will remain active to continue periodic checks.

D. Obstruction Handling and Extended Sleep Mode

If the shading clears and the solar cell receives sufficient light intensity, the system will return to its normal operation. However, if the obstruction continues for more than an hour, the Real-Time Clock (RTC) timer will stop any further wakeups to prevent unnecessary battery drain. This approach ensures energy efficiency and extends the device's operational lifespan under limited power conditions.

IV. Work result

With the selected components and the chosen programming approach, several key outcomes were achieved.

A. Device consumption

The device was designed with a strong emphasis on maximizing energy efficiency. In sleep mode, the device consumes an average of 180 µA, while in positioning mode, the power consumption can increase to as much as 200 mA. Due to this significant difference, it is crucial to execute the positioning process as quickly as possible to minimize energy usage.

B. Charging time

The device was tested on a bright, cloudless day and fully charged within 11 hours. Although this result is not entirely satisfactory, it is important to note that the solar cell used in this project was not very efficient. In the future, the charging performance could be significantly improved by using a more efficient solar cell.

C. Final result

The outcome of this project was a functional solar charging control system that successfully met its objectives. However, some minor issues arose during operation, particularly with inconsistent control between the servo motors. The SG90 servo was controlled by position, while the DS04-NFC was controlled by speed. To improve consistency in the future, it would be beneficial to replace the DS04-NFC with the SG90-HV, a 360-degree position-controlled servo.

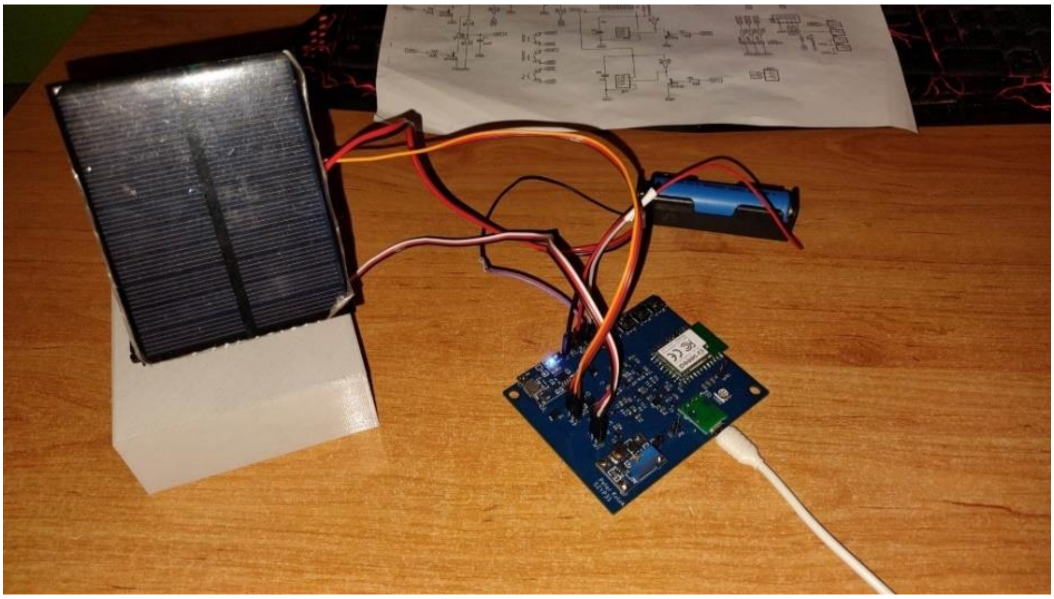

Figure 3. Final application

Additionally, using a more efficient solar cell and programming in a low-level language like C or C++ could enhance both performance and efficiency. Despite these considerations, the project successfully demonstrated the feasibility of positioning a solar cell effectively while charging a Li-ion battery, providing a practical solution for efficient solar charging.

Acknowledgment

"This publication was realized with support of Operational Program Integrated Infrastructure 2014 - 2020 of the project: Intelligent operating and processing systems for UAVs, code ITMS 313011V422, co-financed by the European Regional Development Fund".

EUROPEAN UNION
European Regional Development Fund
OP Integrated Infrastructure 2014 – 2020
MINISTRY
OF TRANSPORT
OF THE SLOVAK REPUBLIC

REFERENCES

[1] A. Maka and J. M. Alabid, "Solar energy technology and its roles in sustainable development," *Clean Energy*, vol. 6, no. 3, pp. 476–483, Jun. 2022.

[2] "The New Stack," *The New Stack*, [Online]. Available: https://thenewstack.io/. [Accessed: 30-Nov-2024].

[3] "Datasheet4U," *Datasheet4U*, [Online]. Available: https://www.datasheet4u.com/. [Accessed: 30-Nov-2024].

[4] "Afrik21," *Afrik21*, [Online]. Available: https://www.afrik21.africa/. [Accessed: 30-Nov-2024].

[5] P. G. V. Sampaio and M. O. Aguirre González, "Photovoltaic solar energy: Conceptual framework," *Renewable and Sustainable Energy Reviews*, vol. 74, pp. 590–601, 2017.

Airship as an Interesting Tool for the Solving of Various ICT Tasks - Design and Implementation of Testing Interface

Matej Jakab, Adrián Kováčik, Michal Hodoň, Peter Ševčík

Abstract**—** This paper deals with the usage of an airship as a tool for solving various tasks of information and communication technologies (ICT). The most common tasks are measurement of air pollution parameters, monitoring and video recording. There is a big potential in energy savings against quadcopters. An airship can do its job multiple longer times compared to the very common quadcopters. This document describes design and implementation of testing interface. Interface is used for testing controlling model of airship from viewpoint of user. Model of airship in Blender application is used for emulating movement of real airship.

Keywords**—** airship, OpenRex, stabilization, accelerometer, magnetometer, tilt compensation, electronic compass, Blender, visualization..

I. Introduction

Nowadays, the utilization of quad- , hexa-, or octacopters (etc.) for different monitor-ing tasks is quite common to many people. However, it is almost impossible to ob-serve an airship. Though a couple of interesting application scenarios was proposed and successfully applied till this time, as mentioned in [1] - [12], due to the implemen-tation feasibility, utilization of robotic airships is still rare. It should be however said, that airships deliver a big potential in energy savings against, e.g. quadcopters. An airship can do its job multiple longer times compared to the very common multicopters. Depending on the used airship size, it can carry sen-sors to measure air pollution parameters or a camera for video recording. The use of an airship equipped with various tools is wide. It can measure the atmosphere, ob-serve traffic or wildlife. One of the commercial uses is to live stream a video of for an example a concert or any other cultural event. Whenever an accident happens, the airship can observe the place surroundings. Stabilization of an airship requires obser-vations of its position. When the airship is set to a position to stay at, and the position has been changed, the stabilization module must detect these changes and react. In this part, we have tested FXOS8700CQ sensor, a magnetometer combined with an accelerometer. We were sending the resulting data to the Blender software to visualize the results.

II. Stabilization

We must think of different cases of problems related to the airship stabilization. Different methods are used for this purpose on the background of tuned sensory subsystem, [13] - [15].

To move the airship, we must know the heading, its pitch and its roll. We must know this, because when we want to move the airship, we must turn the airship using the steering propeller on the back and we must turn the propelling motors to adjust the pitch, too. Then we can move the airship up or down, back or forward. To know the heading, the pitch, the roll we will follow this document. First we will meat the theory, then the practical part.

During an observation mission, the airship must stay on a desired position. If a wind blows or the airship does not stay on the place for any other reason, it must return to that position. To find out the current position we will use a GPS module connected to the main board. Another

Matej Jakab, University of Žilina, Slovak Republic (e-mail: jakab@stud.uniza.sk)
Adrián Kováčik University of Žilina, Slovak Republic (e-mail: kovacik@stud.uniza.sk)
Michal Hodoň, University of Žilina, Slovak Republic (e-mail: michal.hodon@fri.uniza.sk)
Peter Ševčík, University of Žilina, Slovak Republic (e-mail: peter.sevcik@fri.uniza.sk)

case, when the airship will have to get back to a position it was is, when it lost the LTE signal. In that case we must have previous position saved.

Another feature implemented is similar to car parking sensors, but more ultrasonic distance sensors must be used, because we are covering a 3D space instead of the 2D parking system. The driver has two options to choose. First, the airship will stop when the sensors detect a critical distance between the airship and another object. The second option is that the driver is allowed to hit the object. At slower speed, a collision with some other objects is not always damaging. It is because the airship is light, and it floats.

III. Electronic compass

We have decided to use the OpenRex primary platform as the main control unit of airship. The reason is that OpenRex has many sensors including a gyroscope, an ac-celerometer and a magnetometer. We can connect a disc via the SATA interface. To use LTE, here is a PCIE mini slot and a micro SIM slot, on the board. The OpenRex board is running a Linux with a custom file system. FXOS8700CQ Sensor is a magnetometer combined with an accelerometer. The sensor was used together with GPS for the navigation purposes. To keep an eye on the values of the pitch, the roll and the electronic compass head-ing, we visualize the data in the Blender software. We get the data via the USB port, which is connected with the OpenRex board. In the Blender software we run a Python script to read the data and update the rotations of the X, Y, Z axes of a block, which is representing the board. The serial communication must be set correctly on sides, the python script and the C script running on the OpenRex board.

A compass is a device which points to the north. An electronic compass is similar device based on a magnetometer sensor. Using the electronic compass we can figure out which direction and how much is the airship turned from the north. To know in which direction the airship is heading, we have used the sensor FXOS8700CQ sol-dered down on the OpenRex board. We can use this as an electronic compass. Be-cause the accelerometer is here, too, we can tilt compensate the compass, otherwise we would be only able to use the magnetometer compass along a one single plane, and if tilt, the data will not be accurate.

When the airship tilts, the airship axes change. The same happens with the magne-tometer. Because of that, we must tilt compensate the electronic compass. To do so, we apply the formulas using normalized values of the accelerometer. Using these values it is possible to calculate the pitch and the roll of the airship. According to the pitch and the roll values, it is possible to calculate tilt compensated values. However, this will work approximately up to +40 degrees or –40 degrees of the tilt.

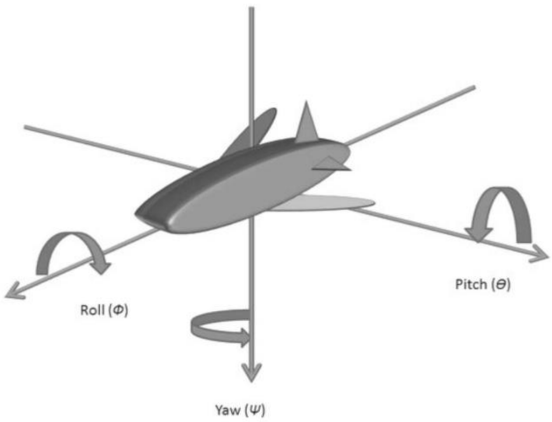

Fig. 1. The Airship Tilt Axes

The source of hard iron distortion is materials, which produce a constant magnetic field. It is additive to the Earth`s magnetic field. For example a permanent magnet or a mag-netic deposit close to the sensor, can produce a hard iron distortion. Soft iron distortion is a distortion coming from materials, which do not generate a direct magnetic field. The materials can have an influence on the Earth`s magnetic field and that way they distorts the magnetic field. It is for example nickel or iron. This distortion is not always a big problem and sometimes it is not needed to filter the soft iron distortion. In the case we are going to filter this distortion, we apply it after the tilt compensation and after the hard iron distortion. The soft iron distortion is more complicated compared to the hard iron, therefore it can´t be removed with a single constant but we need a more complicated filter formula. Magnetic declination is the difference of the magnetic and the astronomic north of the Earth. Here the value is approximately +4,5 degrees, in Žilina. This value must be added at the end to have the correct compass result.

IV. Control algorithm

To read, convert the sensor data into usable units and send it, we are running a C script using an I2C communication interface. We send the data to the PC via a serial communication interface. At the beginning of the program we set up the I2C, the serial port and the sensor registers. If it is needed we have to re-calibrate the magne-tometer. Then, in the infinite loop, we read the register data, correct the data and send them via the serial interface. Here we can see the raw magnetometer and accelerometer output:

```
Magnetometer raw data:
magRawX: 103, magRawY: 250, magRawZ: -293
```

```
Accelerometer raw data:
accRawX: -44, accRawY: 14, accRawZ: 4060
```

Now we are going to work with these raw values to get the heading of the board so we can use it as the compass. If we want an accurate electronic compass, we must apply the following steps:

Calibration - During the magnetometer calibration, to get its maximal and minimal values, we turn the board in all the axes. To skip the calibration next time we use this device, we have to save and use the values. This is guaranteed only if we use the magnetometer at the same place.

Tilt compensation - In the beginning we must calculate the normalized accelerometer data:

```
accNormX = accRawX / sqrt( accRawX2 + accRawY2 + accRawZ2 );
accNormY = accRawY / sqrt( accRawX2 + accRawY2 + accRawZ2 );
```

The normalized values of the accelerometer are close to 0. It is because the OpenRex board is not tilted but it is lying on a flat table:

```
Accelerometer normalized data:
accNormX: -00,01
accNormY: 000,00
```

We calculate the pitch:

```
pitch = asin( accNormX );
```

We calculate the roll:

```
roll = -asin( accNormY / cos(pitch) );
```

We can see the calculated pitch and the roll values lower here:

```
pitch: -00,01
roll: -00,00
```

Now we can calculate the compensated values of the tilted magnetometer:

```
magCompX = magRawX . cos(pitch) + magRawZ . sin(pitch);
magCompY = magRawX . sin(roll) . sin(pitch) + magRawY . cos(roll) - magRawZ
. sin(roll) . cos(pitch);
```

Hard Iron Distortion - To get rid of the hard iron distortion we must apply the following formula:

```
magDataX = magCompX - ( magMinX + magMaxX ) / 2;
magDataY = magCompY - ( magMinY + magMaxY ) / 2;
```

Soft Iron Distortion - Sometimes we must filter the soft iron distortion. To do so, we apply this formula:

```
magDataScaledX = ( magDataX – magMinX ) / ( magMaxX – magMinX ) . 2 – 1;
magDataScaledY = ( magDataY – magMinY ) / ( magMaxY – magMinY ) . 2 – 1;
```

One of the last steps is to calculate the magnetometer heading. Depending on the use of the soft iron filter, we use the variable magData or the magDataScaled:

```
heading = 180 . atan2( magDataY, magDataX ) / 3,14159265;
```

Magnetic Declination - Finally, to correct the heading we must add the magnetic declination to the heading:

```
heading = heading + declination;
```

Lower here we can see the result as the heading of the magnetometer:

Tilt compensated electronic compass with added declination:

```
heading: 066,14
```

Pitch and Roll in Degrees - We can calculate a little bit more. Out from the accelerometer raw data we can calcu-late the pitch and the roll in degrees:

```
angleX = ( atan2( accRawY, accRawZ ) + 3,14159265 ) . 57,29578;
angleY = ( atan2( accRawZ, accRawX ) + 3,14159265 ) . 57,29578
```

We can observe the X and Y angles calculated by the upper formulas:

```
Angles calculated out from the accelerometer raw data:
angleX: 180,20, angleY: 180,62
```

V. TESTING INTERFACE

We decided to use as testing interface, application Blender, which is open source software used for modeling and rendering 3D computer graphic. Another strong as-pect of this application is possibility of writing and executing scripts written in Python programming language and utilization of bpy.py library provided by Blender, which extends abilities of Python programming language by incorporating functions, which provide access to data, functions and tools of program Blender. Testing interface of Blender was used by us to create model of airship.

We didn't come out from any particular specification during process of modeling and for purposes of testing was our airship model very simple. When specification of concrete construction and positions of engines will be known, it is possible to adjust model according specifics. Our designed model is sufficient for emulating purposes. The more important aspects of model as its appearance are model attributes in meaning of Blender application. Each model in Blender is perceived as object in this application with many different attributes, such as size, position, location etc. The most important attributes for us was position and location of object. Position of ob-ject is its relative position in consideration of center of coordinate system defines as point (0,0,0). Our model is depicted at beginning of emulation. Second important attribute of object is rotation of object, which describes position of object in consid-eration of each individual axis x, y, z.

Object interaction is made by user in user interface of Blender application or through execution of Python script, where object and its attributes are accessible with bpy library.

A. Design and implementation of Python script

Script design for controlling movement of virtual airship must fulfill several condi-tions, which we determined. Those conditions were:

- Simple controlling of model airship by utilization of functions, that provides bpy library
- Creation of connection and reading controlling data from primary applica-tion
- Autonomous execution of Python script from the rest of Blender applica-tion, because of fluid execution of this application

Design of script consisted of three main aspects, with which we provided all de-clared conditions. Our designed solution is only one from many, which can be done by Python scripting. This solution is sufficient for purposes of our project and its im-plementation permits later extensions of functionalities. Those three aspects of scripts were definition and implementation of modal operator class, implementation of separated thread and implementation of local TCP/IP server inside that thread.

B. Modal operator class

Class Operator (bpy.Types.Operator) defines class, in which it is possible to create and there are created tools of Blender application. Epithet modal has those tools, which implements function of same name and examples of those tools are transla-tion, rotation and other interactive tools, which are used for manipulation with object and its attributes in real time. Supported by those knowledge and abilities of basic class Operator, we designed inherited class

AirshipOperator, which task was auton-omous controlling of all manipulation with model based on data from external source. Independence and undisrupted execution of operator instructions is provided by keyword return values of each individual function of operator, where each function return value is decided according to inner logic. Relevant keyword return values for us during design were:

- Running modal keyword is used for defining call of method modal(), which is executed parallel with Blender application and its execution is repeated until method is cancelled or task is finished;
- Finished keyword is used to terminate execution of operator, when operator fulfilled its purpose;
- Cancelled keyword is used to terminate execution of operator, when error or exception occurred during execution of one of the function;
- Pass through keyword is passive return value, after which operator waits un-til one of Blender events cause call of modal() function.

Implementation of inherited class AirshipOperator had to contain following func-tions for providing expected functionality:

- Execute() or invoke() functions are used to initialize created object of opera-tor and return value in case correct execution of those function is Running modal;
- Modal() method, which was implemented with translation and rotation in-teraction with object of airship model (for purposes of fluid interaction with user interface of Blender application, we implemented all required reading of controlling data from primary application and processing of all required calculation inside separated thread)

C. Method modal()

Method modal() is called after occurrence of any type of event in application, concretely events, which occur in active window with object. Those event can be caused by inputs from keyboard, mouse or through activation of timer. In execute() method of operator, we registered during initialization of object timer with command, which invokes timer event each 10 milliseconds (timer periodicity can be simply changed according our predefined requirements), and method modal is executed.

```
self.timer = context.window_manager.event_timer_add
(0.01, context.window)
```

Method modal is executed also after invocation by any other type of event, which is cause by other component. It is impossible to influence appearance of other events, but we can filter out other event through condition inside modal method. In the next example, it can be seen snippet of modal method source code, where object attributes of location and rotation are set, in case event type is timer.

```
if event.type == 'TIMER':
bpy.data.objects['Airship'].location =
self.thread.position
bpy.data.objects['Airship'].rotation_euler =
self.thread.rotation
```

As it can be seen from code snippet, we used functionality of bpy library, which made objects and its attributes available. Bpy library consists of different modules. We used several of them in our script and those modules incorporate:

- bpy.context - contains information about actual working environment, such as actual working area, screen, scene, window and window manager ;
- bpy.data - provides access to Blender internal data and objects ;
- bpy.ops - provides python access to calling operators, this includes operator written in C, Python and also our own defined operators ;
- bpy.types
- bpy.utils – contains utility functions specific to Blender but not associated with blenders internal data .

With those abilities of bpy library, it is easily possible to manipulate many different things in Blender application, control and handle several different objects.

D. Thread implementation

We implemented separated thread class standardly, evenly as in Python language, inherited from Python threading.Thread class. Main purpose of implementing thread was to lighten main application from reading controlling data and their processing. Thread class was implemented with several methods with different purport.

1) __init__(self) method: contains initialization of thread object and setting of da-ta variables to initial values,

```
self.position = [0,0,0]
self.rotation = [0,1.57,0]
```

where variable position defines actual position of object in coordinate system and variable rotation is its orientation in consideration of axes. Inchoative value of posi-tion variable is center of coordinate system, where emulation starts. Unit, in which variable elements are indicated, is internal unit of measurement in Blender applica-tion. Initial value of rotation variable sets object to horizontal and lateral orientation in consideration of user viewpoint. To achieve that, we had to set initial offset of 1,57 (or $\pi/2$) radian to Y axis. Rotation variable elements are in radian unit.

2) start(self) method: contains assignment of positive value to running variable, which stores information about thread activity and it is accessible from main applica-tion thread. Second task of method is starting thread itself.

3) stop(self) method: contains assignment of negative value to running variable, which has impact to existence of thread. Method is called from main application thread, when emulation is over.

4) run(self) method: contains all thread logic and incorporates while loop, which maintains and executes thread commands. Essential tasks of method are:

a) Communication: Creation and maintaining of local TCP/IP socket server, on which primary application connects and sends controlling data

b) Data reading: Data are read in periodic intervals and temporary stored be-fore processing and transformation, in form of data packet, which contains con-trol data. We defined data packet in simplified way, which is sufficient for purpos-es of emulating movement. Implementation of more complicated moveset in-cludes redesign of data packet and processing of new data. Content of our data packet and meaning of its elements is:

Data packet			
Direction axis movement data	*Altitude* axis movement data	*Translation* movement data	*Translation* movement data

• First data packet element (Direction data) contains information about ob-ject movement in horizontal axis given the surface

• Second data packet element (Altitude data) contains information about ob-ject movement in vertical axis given the surface, ascending or descending of whole object or its part, which depends on behavior of real airship model

• Third and fourth packet elements (Translation data) contain instruction for initialization or continuation of object translation movement forward, where all attributes of position and rotation are used to determine movement in coordinate system.

Data elements in data packet are separated with colon, which is used to ascer-tain each element independently. Each data element value is from range <0,100>. Direction and altitude data elements passive value is 50, where increment or dec-rement of this value leads to rotation movement. Translation data elements pas-sive value is 0, where its increment lead to translation movement forward.

c) Data transformation: Processed data packet is used for transformation into object movement in Blender environment. First and second data elements con-tains exact requirement for rotation in one corresponding axis. Value of data ele-ment is used to determine direction and length of rotation. Rotation movement and altitude regulation of model object are done through modification of its rota-tion attribute in corresponding axis.

```
if int(dataElem[0]) <= 20:
self.rotation[2] += 0.01
if int(dataElem[0]) > 20 and int(dataElem[0]) <= 40:
self.rotation[2] += 0.005
```

Processed data from data packet are stored in dataElem array variable and ac-cording their value transformed to object rotation in one concrete axis. Change of rotation attribute is small, because of high frequency of repeating control data read-ing and their transformation. Translation movement forward is more complicated, due to fact that object movement occurs in tridimensional space, which means in each of its axes. Resulting translation line depends on initial position of object and its orientation in consideration of axes. We implemented calculation of such movement through goniometric functions,

```
self.position[0] -= 0.006 * math.cos(self.rotation[1] -
1.57) * math.cos(self.rotation[2])
self.position[1] -= 0.006 * math.cos(self.rotation[1] -
1.57) * math.sin(self.rotation[2])
self.position[2] += 0.006 * math.sin(self.rotation[1] -
1.57)
```

where position array defines actual position of object in all axes and new position is calculated through goniometry with consideration of actual orientation of object.

E. Local TCP/IP socket server implementation

One of the reasons, why we chose application Blender as core application for our testing interface and emulation of airship movement was possibility to utilize script-ing with Python language. Primary application used by user is defined in real situation as client and software on real airship as server, on which client connects. We could define communication interface with equivalent attributes in testing interface, through Python scripting and implementation of local TCP/IP socket server with equally to server interface on airship. This way, we comprehended in our design not only emulation of airship movement, but also simplified emulation of communica-tion interface. Server is defined as TCP/IP socket communication, through stream.

```
s = socket.socket(socket.AF_INET,socket.SOCK_STREAM)
s.bind(('127.0.0.1', 9013))
```

Server listens on localhost adress (‘127.0.0.1’) and waits for connection from primary application on same computer, which features as client part of communi-cation interface.

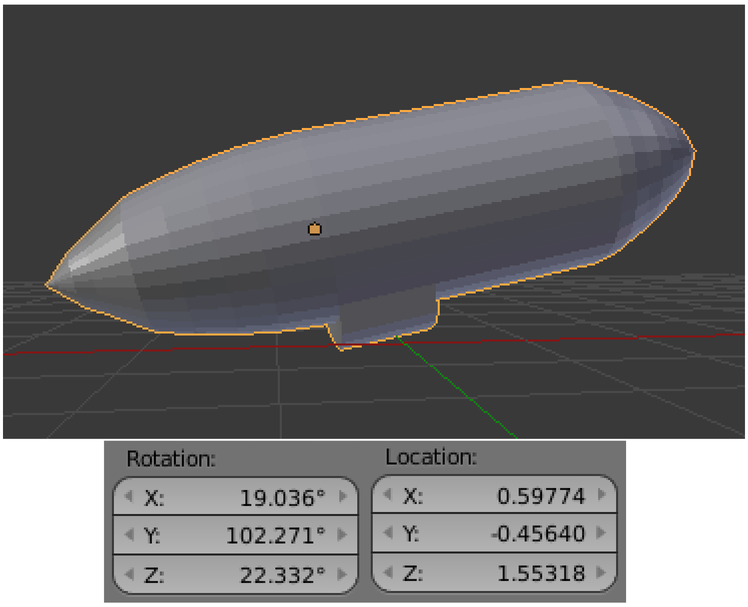

Fig. 2. Airship model in Blender application and attributes of rotation and location

VI. Conclusion

Introduced testing interface was successfully implemented and verified. It will be used as the simulation tool with the possibilities of quick proof of different control policies applicable for the airship movement. Such tool will significantly save costs during the development process of the airship navigation algorithm. It also open an-other options for integration of different physical models which could improve the simulation scenario to be as close to the real conditions as possible. Portability of the system allows easy transmission of developed algorithms between virtual world and the airship with mentioned control unit.

Acknowledgment

"This publication was realized with support of Operational Program Integrated Infrastructure 2014 - 2020 of the project: Intelligent operating and processing systems for UAVs, code ITMS 313011V422, co-financed by the European Regional Development Fund".

EUROPEAN UNION
European Regional Development Fund
OP Integrated Infrastructure 2014 – 2020

MINISTRY
OF TRANSPORT
OF THE SLOVAK REPUBLIC

REFERENCES

[1] Y.-b. Li and X. Wang, "Ground station software design of tethered air-ship monitoring system," *2011 International Symposium on Computer Science and Society*, IEEE, Kota Kinabalu, Malaysia, Jul. 16-17, 2011, DOI: 10.1109/ISCCS.2011.99.

[2] A. Elfes, S. S. Bueno, M. Bergerman, and J. G. Ramos, "A semi-autonomous robotic airship for environmental monitoring missions," *IEEE International Conference on Robotics and Automation*, Leuven, Belgium, May 20, 1998, DOI: 10.1109/ROBOT.1998.680971.

[3] J. J. SantaPietro, "Persistent wide area surveillance from an airship," *IEEE Aerospace and Electronic Systems Magazine*, vol. 27, no. 6, pp. 10-16, Jun. 2012, DOI: 10.1109/MAES.2012.6328548.

[4] K. Izet-Ünsalan and D. Ünsalan, "A low cost alternative for satellites - tethered ultra-high altitude balloons," *5th IEEE International Conference on Recent Advances in Space Technologies*, Istanbul, Turkey, Jun. 9-11, 2011, DOI: 10.1109/RAST.2011.5966806.

[5] T. Xu, X. Zhang, and Y. Lu, "Onboard controlling system design of unmanned airship," *International Conference on Electronic and Mechanical Engineering and Information Technology IEEE*, Harbin, Heilongjiang, China, Aug. 12-14, 2011, DOI: 10.1109/EMEIT.2011.6023728.

[6] Y. Liu, Z. Pan, D. Stirling, and F. Naghdy, "Control of autonomous airship," *IEEE International Conference on Robotics and Biomimetics*, Guilin, China, Dec. 19-23, 2009, DOI: 10.1109/ROBIO.2009.5420403.

[7] M. Galletti, G. Krieger, T. Borner, N. Marquart, and J. Schultz-Stellenfleth, "Concept design of a near-space radar for tsunami detection," *IEEE International Geoscience and Remote Sensing Symposium*, Barcelona, Spain, Jul. 23-28, 2007, DOI: 10.1109/IGARSS.2007.4422723.

[8] H. A. Kadir and M. R. Arshad, "The development of unmanned small-size double hull blimp for low altitude surveillance system," *IEEE International Conference on Underwater System Technology: Theory and Applications*, Penang, Malaysia, Dec. 13-14, 2016, DOI: 10.1109/USYS.2016.7893922.

[9] D. Gobiha and N. K. Sinha, "Autonomous maneuvering of a stratospheric airship," *IEEE Indian Control Conference*, Kanpur, India, Jan. 4-6, 2018, DOI: 10.1109/INDIANCC.2018.8307998.

[10] P. Sun, X. Wang, and W. Xie, "Centrifugal blower of stratospheric airship," *IEEE Access*, vol. 6, pp. 11516-11524, Feb. 27, 2018, DOI: 10.1109/ACCESS.2018.2809707.

[11] G. Franceschetti, V. Gervasio, and F. Vinelli, "Large urban areas monitoring: Use of unmanned microwave powered airships as remote sensing nodes," *International Microwave Workshop Series on Innovative Wireless Power Transmission: Technologies, Systems, and Applications*, Kyoto, Japan, May 10-11, 2012, DOI: 10.1109/IMWS.2012.6215796.

[12] J. Zahour, L. Elis, J. Krivka, P. Stetka, and K. Kosturik, "Control unit of monitoring airship and its communication interface," *21st Telecommunications Forum*, Belgrade, Serbia, Nov. 26-28, 2013, DOI: 10.1109/TELFOR.2013.6716298.

[13] J. Wang and M. Xiuyun, "Active disturbance rejection backstepping control for trajectory tracking of the unmanned airship," *IEEE International Conference on Unmanned Systems*, Beijing, China, Oct. 27-29, 2017, DOI: 10.1109/ICUS.2017.8278379.

[14] B. Chen, "Adaptive backstepping sliding mode tracking control for the stratospheric airship," *12th International Conference on Computer Science and Education*, Houston, TX, USA, Oct. 30, 2017, DOI: 10.1109/ICCSE.2017.8085489.

[15] F. Ben Abdallah, N. Azouz, L. Beji, and A. Abichou, "Modeling and stabilization of a cable-driven parallel platform suspended by an airship," *11th International Workshop on Robot Motion and Control*, Wasowo, Poland, Jul. 3-5, 2017, DOI: 10.1109/RoMoCo.2017.8003892.

[16] P. Herman and W. Adamski, "Nonlinear tracking control for some marine vehicles and airships," *11th International Workshop on Robot Motion and Control*, Wasowo, Poland, Jul. 3-5, 2017, DOI: 10.1109/RoMoCo.2017.8003922.

[17] C. Blouin, E. Lanteigne, and W. Gueaieb, "Optimal control for the trajectory planning of micro airships," *International Conference on Unmanned Aircraft Systems*, Miami, FL, USA, Jun. 13-16, 2017, DOI: 10.1109/ICUAS.2017.7991324.

[18] C. Nie, M. Zhu, Z. Zheng, and Z. Wu, "Model-free control for stratospheric airship based on reinforcement learning," *35th Chinese Control Conference*, Chengdu, China, Jul. 27-29, 2016, DOI: 10.1109/ChiCC.2016.7555054.

Modernization of the Transport Laboratory

Ondrej Karpiš, Peter Ševčík, Veronika Olešnaníková

Abstract**—**The education of students at universities is based not only on the transfer of theoretical knowledge, but also on its application in practice. During the teaching of students at the Faculty of Transport and Communications Operations and Economics of the University of Žilina, the transport laboratory has been used for more than 25 years to practise practical skills. Since 2020, its complete reconstruction has been underway. This article describes the main changes implemented during the modernization, particularly the change of the topology of the model railway, its digitisation and the renewal of conventional types of interlocking equipment.

Keywords**—**laboratory modernization, practical education, railway model

I. INTRODUCTION

In the process of education of students at the university it is important not only to acquire theoretical knowledge but also its practical application. Employers are also interested in graduates with practical experience. Connecting education with practice is possible in various ways - in the form of lectures by people from practice, excursions or internships directly in companies. Thanks to the development of digital technologies, it is sometimes possible to try out working with real equipment through virtual reality. But it is best if students can work on the same equipment as is used in practice. In some cases, it is not possible to make a life-size copy of the system - then a scale model must be used. Such systems include railway traffic control.

To improve the quality of teaching of students in various fields of study, a transport laboratory was built at the Department of Railway Transport at the Faculty of Operation and Economics of Transport and Communications of the University of Žilina. It was put into operation in 1994. For 25 years it allowed students to get acquainted with the construction and operation of railway interlocking equipment used in the network of the Railways of the Slovak Republic (ŽSR) and to practice theoretical knowledge related to the management of railway transport - the organisation of train running in stations and inter-station sections, train formation, management of local work in stations, etc. The laboratory is also used in the preparation of ŽSR employees for the theoretical part of qualification professional examinations and in regular retraining of employees. Moreover, the laboratory has been used extensively for marketing purposes of the department, faculty and the entire university practically since its construction. Numerous excursions of children and students of primary and secondary schools have taken place in the laboratory when presenting the possibilities of studying at the University of Žilina, especially within the framework of the Open Day and the regular Žilina Children's University.

Since its inception, the laboratory has been heavily used. Thanks to regular maintenance, most of the control systems were still functional after almost 27 years. The increased failure rate of the systems in the laboratory, as well as the need to extend the laboratory technology with new modern systems, which at the time of the laboratory construction had not yet been developed and deployed in the ŽSR network, led to a complete reconstruction and modernization of the laboratory.

Ondrej Karpiš, University of Žilina, Slovak Republic (e-mail: ondrej.karpis@fri.uniza.sk)
Peter Ševčík, University of Žilina, Slovak Republic (e-mail: peter.sevcik@fri.uniza.sk)
Veronika Olešnaníková, University of Žilina, Slovak Republic (e-mail: veronika.olesnanikova@fri.uniza.sk)

II. THE ORIGINAL TRANSPORT LABORATORY

The original transport laboratory consisted of five stations and their respective track sections. The following station interlocking equipment (SIE) were emulated in the stations:

- Hričov station: relay SIE type AŽD 71 with travel option,
- Púchov station: relay SIE type AŽD 71 with digital selection,
- Vrútky station: electromechanical SIE model 5007,
- Bytča station: relay SIE type TEST 14,
- Žilina station: electronic interlocking of unspecified type.

The following systems were emulated as track interlocking equipment (TIE): two-way automatic TIE type AH 71, two-way automatic TIE type AB 3-82 and two-way semi-automatic TIE type RPB 71.

In addition to the stations, a dispatcher's station was also implemented, which enabled remote control and remote operation of the stations - construction and cancellation of simple paths and simulation of faults.

The movement of the trains in the model track was realized by connecting traction voltage to the track sections. This method of motion control did not allow to realize all traffic activities that take place in real stations (e.g. driving of working trains on the line with return to the starting station). Two levels of traction voltage were used, corresponding to two different vehicle speeds. Thus, the system did not allow a smooth voltage control, and it was not possible to achieve a faithful dynamic of the trains movement on the track.

The control system of the transport laboratory was conceived as a distributed system - each station had its own control computer, which controlled the components of the model track (control of the position of exchanges, control of light signals, control of the model vehicles and detection of the presence of vehicles in individual track sections) and at the same time modelled the behaviour of the relevant type of station or track interlocking equipment in the station or inter-station section. The basic task of the control system was to model the behaviour of control and indication elements of all interlocking systems in accordance with the specification of individual signalling devices and the requirements of the valid ŽSR regulations.

The control system of each station consisted of a PC AT 286 control computer, expanders and input/output modules. The expanders allowed up to 16 I/O modules to be connected to the computer bus. The input module allowed the input of 24 binary information, with an input voltage magnitude in the range of 5-24 V representing logic 0. All inputs were optically isolated. The output module allowed the output of 24 binary information. Each output was controlled by an optically isolated transistor and allowed switching voltages up to 32 V with current up to 75 mA. The power version of the output module allowed to permanently switch currents up to 500 mA. The traction voltage control was implemented by a power module with current protection. The module allowed to control 12 isolated sections by connecting positive or negative voltage for forward and reverse motion of trains.

III. THE ORIGINAL TRANSPORT LABORATORY

The original technology used in the transport laboratory has been in operation for over 25 years. In that time, it has become morally and technically obsolete. The physical obsolescence of the control system was manifested by increasingly frequent failures, which eventually caused the complete non-functionality of the Púchov station and the partial non-functionality of the Vrútky station. During the operation of the laboratory, flaws in the original design of the track topology were also identified:

- insufficient number of inter-station sections,
- the absence of a model of the level crossing interlocking equipment,

- the use of a model of an unspecified type of electronic interlocking,
- the absence of a system for remote control of traffic in the intermediate station section.

During the modernization of the transport laboratory, the topology of the model track was modified by adding additional railway stations and inter-station sections, while maintaining the concept that individual railway stations are controlled by a different type of station interlocking equipment. Figure 1 shows topology of the modernized track.

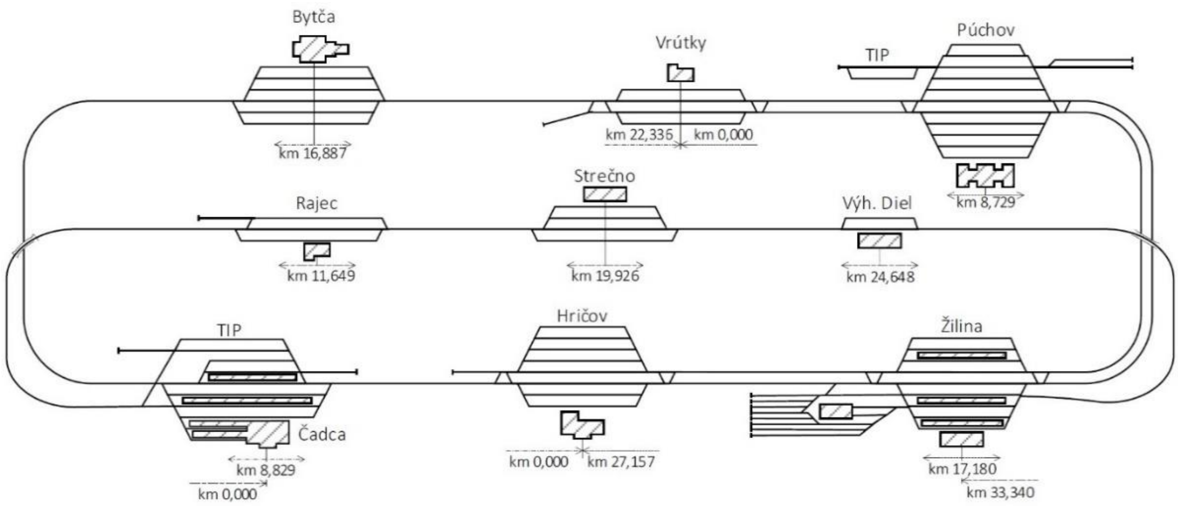

Figure 1 Topology of the modernized track

To enable the training of traffic dispatching, a new single side track was built between the stations Čadca and Žilina, which is centrally controlled by the system of remote control and checking of interlocking equipment. In addition to the increase in the number of stations, the modernization also changed the type of some interlocking equipment. The stations with relay and electromechanical station interlocking remained unchanged. The following types of station interlocking equipment are used in the other stations:

- Žilina station: SIMIS W electronic interlocking with ILTIS supervisory system of SIEMENS Mobility. The ILTIS supervisory system allows to display the station track on one to eight colour monitors, depending on the size of the station, while the used catalogue of symbols of the elements in the track and the displayed traffic situations is implemented in accordance with the valid regulations of ŽSR [1-3].
- Čadca station: a newly built railway station with ESA 44 electronic interlocking of AŽD Praha. The method of controlling the interlocking by means of a mouse and displaying the operating statuses is implemented in accordance with [4].
- Rajec station: newly built railway station secured by electronic interlocking type ESA 44 remotely controlled from the control station Strečno.
- station Strečno: newly built railway station secured by electronic interlocking type ESA 44. The station will remotely control both Rajec station and Diel switching station.
- Switching station Diel: a newly established transport station secured by electronic interlocking
- type ESA 44 remotely controlled from the control station Strečno.

Track interlocking equipment has also been updated to match the most used types of interlocking equipment in Slovakia. Currently the following systems are implemented: automatic block ESA-ITZZ, automatic gate ESA-ITZZ, automatic block AB3-88, automatic block AB3-74/88, relay semi-automatic block RPB 71 and centralized automatic block ABE-1.

A. Model railway

The model railway has been fully digitised. It is built on commercially available equipment using DCC and XpressNet communication protocols. The model railway uses switch control modules, feedback modules, signal modules and DCC signal boosters. All turnouts in the model railway are electromagnetic. The modelling of the lower speed of the real turnouts is implemented by delays in the control computers. The communication of the control computers with the station elements is provided by Ethernet/XpressNet converters. The digitisation of the track and trains allows not only to model more faithfully the behaviour of the trains (smooth starting and braking, lights and sounds) but also to model situations that could not be realised in the original system (e.g. two trains on the same track).

B. Renewal of conventional types of interlocking equipment

Conventional interlocking equipment (i.e. relay and electromechanical) is characterised by the use of a specialised control and indication panel. The control system shall provide a faithful simulation of the response of the system to the operation of the controls located at the control panel, to the operation of the controls in adjacent stations related to the operation of trains in the inter-station section, and to the various operational situations in the model track of the station and adjacent track sections, with the response of the indicating elements corresponding to the type of station or track interlocking equipment modelled. A faithful simulation of the behaviour shall also be ensured by the control system when simulating selected fault conditions of the relevant type of interlocking equipment.

The renewal of conventional interlocking equipment, including the software, was carried out by the Department of Technical Cybernetics at the Faculty of Management and Informatics. Due to the very good condition of the original cabling in the control panels, it was decided to replace only the input/output boards and the communication subsystem. To minimize the required cabling between the operator panel and the control computer, the CAN bus was chosen as the communication interface. The input and output boards are based on the XYZ microcontroller, which contains enough I/O pins and has built-in support for CAN communication. Dimensions, location of connectors, and mounting holes of developed boards are compatible with the original boards.

The new boards also contain indicator elements (LEDs) that allow visual control of the current status of all inputs or outputs. Instead of screw terminals, plug-in connectors have been used to simplify the replacement of the board in case of failure. Each board also contains a small EEPROM memory in which the board settings, especially the board address, are stored. Address configuration is accomplished by sending a defined CAN message when a user button is pressed.

The control program was created in C++ and is designed for the Windows operating system. It mainly provides modelling of the relevant type of station and track interlocking equipment, as well as simulation of fault conditions. The software also allows testing of all elements in the model railway and in the control panel. In a separate window it is possible to monitor the status of station elements, i.e. the status of turnouts, occupancy of sections and the status of signals. In another window, a digital copy of the control panel can be displayed (Figure 2), which shows the status of all indicating and control panel elements and allows to emulate the use of the controls. Thus, control of the station is possible even in the event of a control panel failure. The program also allows the activation of the simulation mode, in which it is possible to simulate the behaviour of the model station, including the train running. The software can therefore also be used independently as a simulation tool for students to practice their practical skills individually.

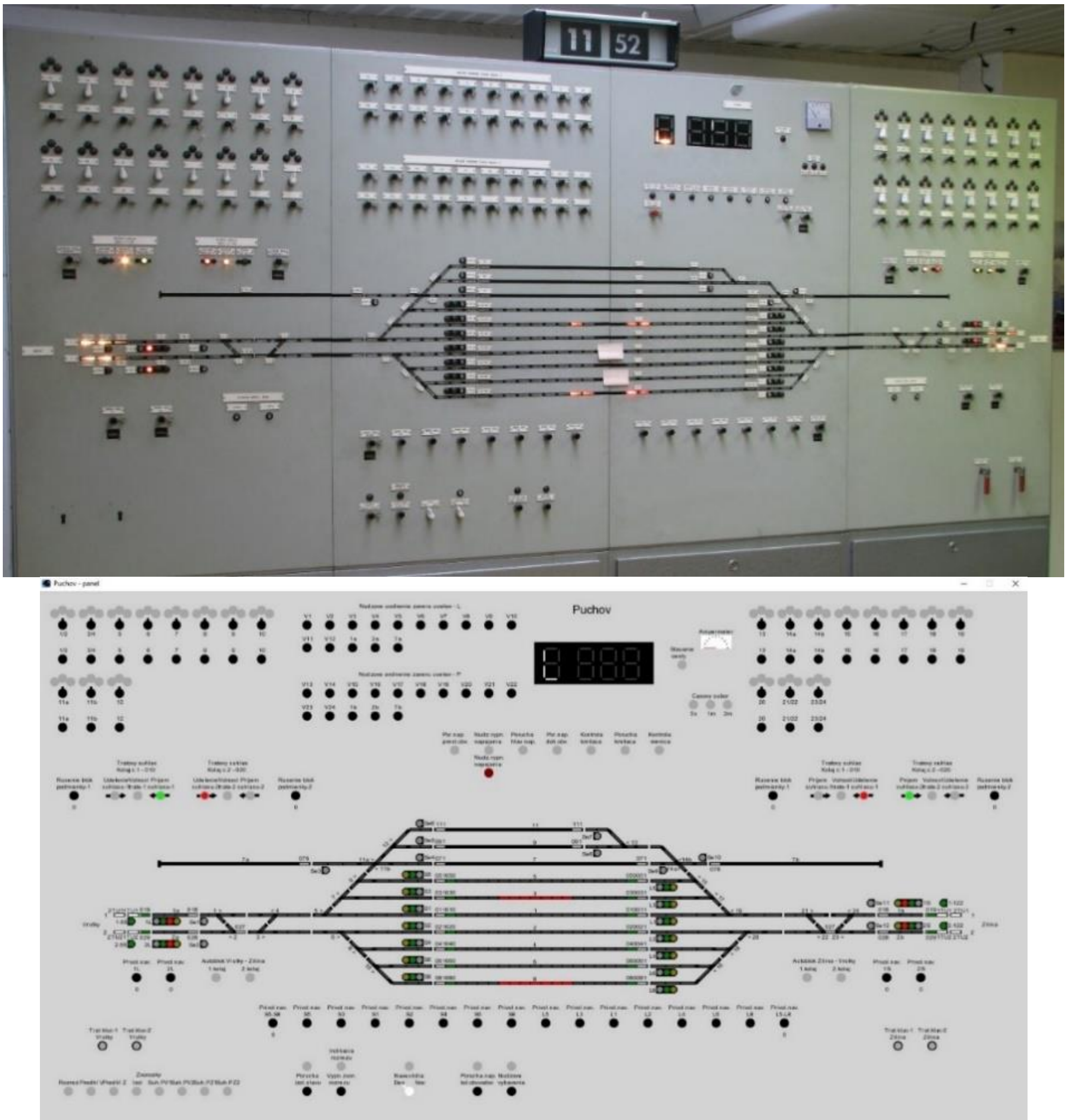

Figure 2 Control panel of the station Puchov and its digital copy

References

[1] Železnice Slovenskej republiky, *D101/T101-O 420-2010: D101/T101 – Príloha 8a – Predpis Obsluha staničných zabezpečovacích zariadení, Zmena č. 4: Obsluha elektronického stavadla typu SIMIS W, Popis činnosti*, účinnosť od 01.07.2009.

[2] Železnice Slovenskej republiky, *D101/T101-O 420-2010: D101/T101 – Príloha 8b – Predpis Obsluha staničných zabezpečovacích zariadení, Zmena č. 4: Obsluha elektronického stavadla SIMIS W, Spôsob obsluhy*, účinnosť od 01.07.2009.

[3] Železnice Slovenskej republiky, *D101/T101-O 420-2010: D101/T101 – Príloha 8c – Predpis Obsluha staničných zabezpečovacích zariadení, Zmena č. 4: Obsluha elektronického stavadla SIMIS W, Symboly zobrazovania*, účinnosť od 01.07.2009.

[4] Správa železniční dopravní cesty, *ZTP 5/2000 Základní technické požadavky. Jednotné obslužné pracoviště. Vydání IV.*, účinnosť od 01.05.2000.

Solar Car: Example of Low Power Design

Juraj Miček, Peter Ševčík, Michal Hodoň

Abstract**—**The paper outlines the problems associated with the increasing energy consumption of ICT (Information and communications technology) devices as well as their overall environmental footprint. Even though the area of embedded systems is not dominant in terms of energy consumption, it is necessary to highlight the need for their energy efficient design. IoT (Internet of Things) and WSN (Wireless Sensor Networks) devices are specific in that they most often operate off the power grid. Their long-term operation is ensured by batteries, often supplemented by ambient energy harvesting systems. As an example of a device based on a supercapacitor and a solar cell, a Solar Car is given, which was developed mainly to popularize the study of ICT and to demonstrate selected green computing issues.

Keywords**—**Energy harvesting, Energy management, Green computing, Solar car, Supercapacitor.

I. Introduction

"ICT sector represents ~4 % of global electricity consumption in 2020. The ICT sector represents 1.4 % of global GHG emissions in 2020. User devices represent a majority of GHG emissions (~57 %). Embodied emissions represent 36 % of total emissions. The ICT sector has increased its emissions by about 5 % from 2015." [1]

Based on [1], it can be concluded that the ICT sector consumed approximately 4 % of the global electricity production in the use phase in 2020 and accounted for approximately 1.4 % of global greenhouse gases (GHG) emissions. Electricity consumption in the operation of ICT equipment and overall GHG emissions have increased since 2015. User equipment accounted for more than half of all GHG emissions, with equal shares for the use phase and other life cycle phases. For networks and data centers, the use phase dominates. In [2], it is stated that data centers currently consume a huge amount of energy. The Covid-19 pandemic has triggered an increased need for digital information transfer. Hybrid work is moving much more data to the cloud. Currently, the ICT sector accounts for 7 % of global electricity consumption. Many forecasts signal continued exponential growth in data traffic and the share of emissions produced by ICT is set to rise to 14 % of global emissions by 2040. The rise in energy prices over the last two years has caught the attention of large corporations. The current energy crisis, exacerbated by regional conflicts, has pushed up the price of electricity as well as other forms of energy to their highest level in 100 years. This has contributed significantly to optimizing the operation of generation systems and to lower electricity consumption.

Currently, there is controversy about the possible increase in energy consumption in the ICT sector due to the intensive use of artificial intelligence (AI) tools [3]. Most authors do not expect a dramatic increase in electricity consumption in the coming years due to the advent of AI. It should be noted that a comprehensive assessment of the environmental impact of ICT devices needs to consider their entire life cycle, from production through operation to termination or recycling.

Even though the largest electricity consumption is represented by user computers, data centers and network equipment, it is necessary to address the energy efficiency of other ICT systems such as embedded systems, Internet of Things, wireless sensor network elements, etc. The present paper focuses specifically on the area of embedded systems and devices from the

Juraj Miček, University of Žilina, Faculty of management science and informatics, Žilina, Slovakia (e-mail: juraj.micek@fri.uniza.sk).
Peter Ševčík , University of Žilina, Faculty of management science and informatics, Žilina, Slovakia (e-mail: peter.sevcik@fri.uniza.sk).
Michal Hodoň, University of Žilina, Faculty of management science and informatics, Žilina, Slovakia (e-mail: michal.hodon@fri.uniza.sk).

IoT and WSN domain.

II. EMBEDDED SYSTEMS – POWER SUBSYSTEM

The area of embedded systems is very important in terms of electricity consumption. Due to the huge number of installations, the reduction of energy consumption as well as of the materials used to produce them is significant. Often embedded systems are intended to control other devices and technological units, it is necessary to pay maximum attention during their development to optimize the energy consumption of the entire final installation.

IoT and WSN devices, unlike data centers, are often operated outside the reach of standard power grids. This fact places special requirements on the power subsystem of these devices. In practical applications, we mainly encounter the use of:

- primary power cells,
- secondary power cells,
- energy harvesting systems, in cooperation with secondary energy cells or supercapacitors.

Let us compare the properties and parameters of primary and secondary cells. Primary cells are also known as disposable cells. In primary cells, electrochemical energy is generated by the decomposition of electrodes and electrolytes. The electrochemical reactions taking place in the cell are irreversible. Therefore, it is necessary to replace the primary cell with a new one when it is discharged. Alkaline manganese, silver/zinc oxide, lithium/manganese dioxide and thionyl chloride are some common components of primary cells. Primary cells are expensive and not environmentally friendly as they need to be disposed of at the end of their useful life. They use chemical reactions that are generally not reversible. Once the chemical components are exhausted, the battery stops producing electricity. For example, in alkaline batteries, zinc and manganese dioxide react to produce a flow of electrons until one of the reactants is completely consumed.

Secondary cells are also known as rechargeable cells, these electrochemical cells can be recharged repeatedly. These cells find application in areas where the electrical potential in terms of specific power and specific energy seems to have reached a limit with current state-of-the-art primary lithium-ion batteries. Reversibility of secondary cells is achieved by various chemical processes such as the movement of lithium ions between the anode and cathode in lithium-ion batteries. The ability to reverse this reaction makes these batteries rechargeable.

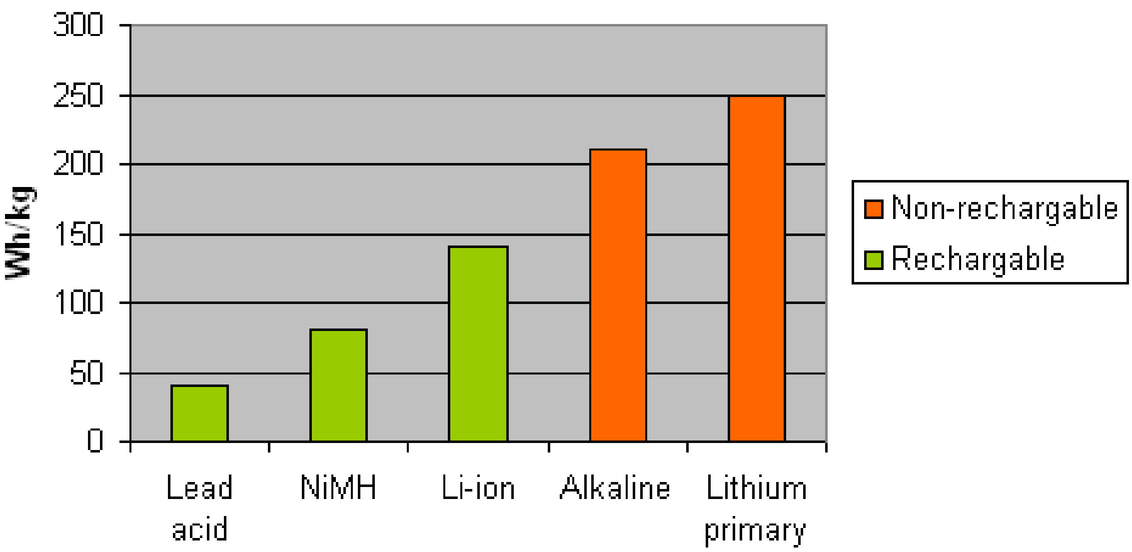

Fig.1 Gravimetric energy density Wh/kg, [5]

In general, primary batteries have a higher energy density than rechargeable batteries, which means they store more energy with respect to their size or weight, as shown in Fig.1. Primary batteries are cheaper per unit of energy but can be more expensive in the long run due to the need for frequent replacements. Secondary batteries, although initially more expensive, can be more economical over time due to their rechargeability. Primary batteries can provide a theoretical energy density 1.5 to 5 times higher than secondary batteries [4]. Primary batteries are typically used in applications where long lifetime is required. Secondary batteries, due to their rechargeability, are suitable for long-term applications despite having a lower energy density.

Supercapacitors store energy through two mechanisms: electrostatic and electrochemical. In electrostatic storage, charge separation occurs at the electrode-electrolyte interface, leading to the formation of an electrical double layer of ions. This double-layer capacitance stores energy without any chemical reactions inside the cell. The energy stored in this way can be quickly released when needed. The electrochemical mechanism involves redox reactions where charge is stored by the movement of ions between the electrolyte and the electrode. Supercapacitors may use one or both mechanisms.

Supercapacitors store much less energy per unit volume or mass compared to conventional batteries. Supercapacitors can deliver a large amount of energy in a short time, making them ideal for applications requiring fast energy consumption. Such applications are, for example, the rapid acceleration of electric vehicles, or camera flashes. Supercapacitors typically have a higher cost per watt. They discharge energy very quickly and therefore can be inefficient in some applications.

Batteries have a much lower self-discharge rate compared to supercapacitors. Thus, batteries are more suitable for applications requiring long-term energy storage without frequent recharging. In batteries, a chemical reaction corrodes the components - so while supercapacitors can handle more than 1,000,000 charge/discharge cycles, a conventional rechargeable battery will only last about 2,000 to 3,000 cycles. The mining of lithium, nickel and cobalt, which are needed for lithium-ion batteries, raises environmental concerns about waste and pollution. In contrast, supercapacitors can use more sustainable materials, such as activated carbon from biomass sources, which are more renewable, less harmful to the environment, and easier to recycle, [6].

Energy harvesting is a relatively new technology for harvesting energy from the environment. Energy harvesting should be defined as the collection of local naturally available energy for local use. Most often energy harvesting systems are small-scale systems with small amounts of energy with power ranging from nanowatts to hundreds of milliwatts. The main area of application is wireless devices. The applicability of energy harvesting to specific devices depends on the type and amount of ambient energy available, as well as size constraints. Motion, temperature gradients, light, electromagnetic radiation, and chemical energy can all be used as sources for energy harvesting. Three different mechanisms are available for motion using electromagnetic, electrostatic or piezoelectric principles. Thermal systems use the thermoelectric effect (also known as the Seebeck effect), light systems use the photoelectric effect, while electromagnetic energy harvesting systems use induction. Chemical systems can use various chemical reactions on the surface of electrodes, etc. A more detailed discussion of the principles and applications of ambient energy harvesting systems is well developed in the literature [7, 8].

When designing the power subsystem of the device under development, it is necessary to select the optimal power supply method while respecting all constraints arising from future operation and economic requirements.

In a second step, it is essential that the whole system is designed to minimize the overall power consumption and to operate in an energy efficient manner. Minimizing power consumption is often a fundamental task in device development. It is often necessary to ensure the long-term operation of systems without operator intervention (electronic labels, heat and water metering systems, and possibly other applications from IoT and WSNs). However, energy efficiency touches every device today, so it is necessary to pay increased attention to addressing this issue.

It should be noted that the energy efficiency of the whole system needs to be addressed at both hardware and software level. The above-mentioned efforts towards energy efficiency and minimizing the ecological footprint of ICT systems are now often referred to as "Green Computing". Geen Computing is of particular importance in the development of IoT devices and WSNs as we are dealing with limited energy resources while maintaining long autonomous operation times [9].

We want to highlight the importance of energy-optimal design of electronic devices with the project "Solar Car", which was previously developed in our department.

III. Solar Car Project

The Solar Car project was created to support the teaching of embedded systems programming. Using the example of energy-efficient application development, the project addresses a range of issues that a developer will encounter in the process of developing a device. The Solar Car is powered only by a solar panel and a supercapacitor. The car is shown in Fig.2.

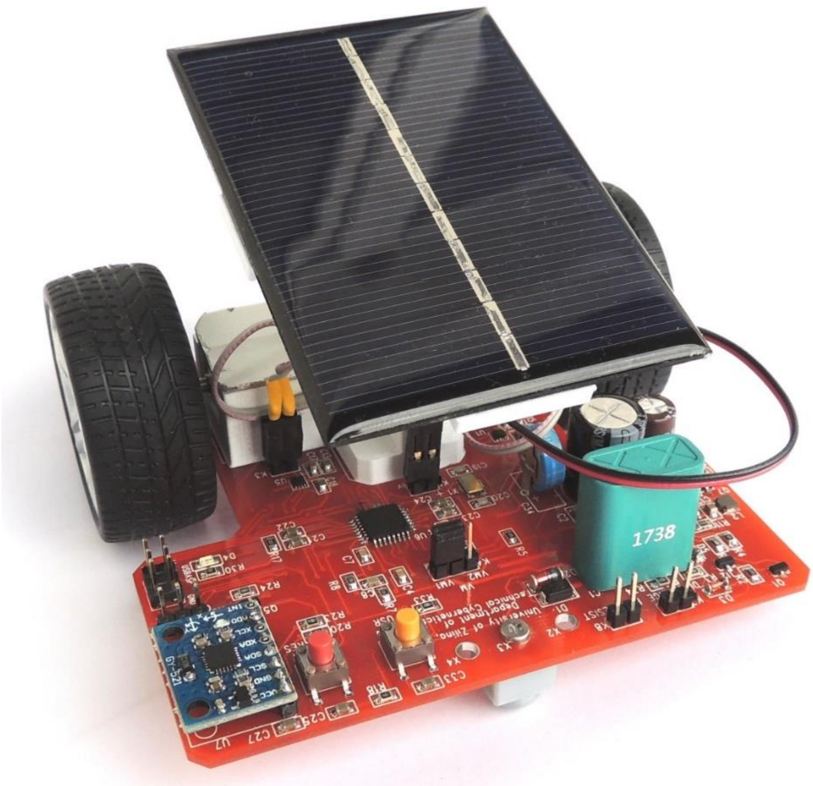

Fig.2 Solar Car

We will briefly describe the circuit design of the Solar Car. Fig.3 shows the block structure of the power supply circuits of the Solar Car. The supercapacitor C1 is charged gradually from the solar panel. It is used to store energy. When the voltage across its electrodes reaches a value of approximately 1.4 V, the DC/DC converter starts working, which increases the input voltage to 3.4 V. This voltage is then used to power all the circuits, including the microcontroller (MCU). This is all implemented by circuit means.

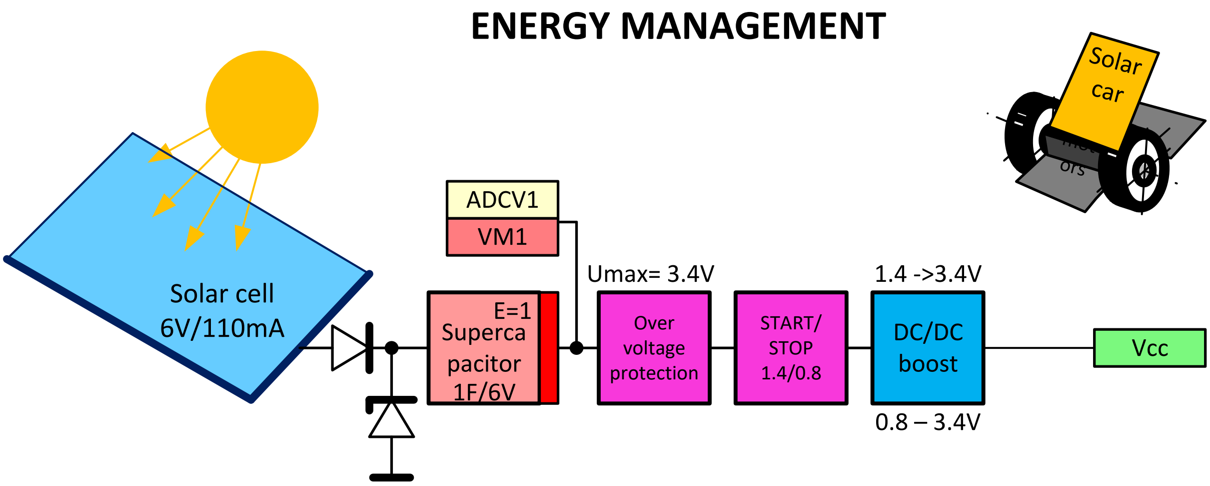

Fig.3 Block structure of Solar Car power supply circuits

From the moment the DC/DC converter starts working, the further operation of the Solar Car can be controlled by the program to minimize the power consumption and at the same time accomplish the task at hand. The control circuits of the car can also be powered via the USBASP programmer from the USB port of the computer. This method of powering the car is used during program development and debugging.

In addition to the power supply circuits, the Solar Car includes a microcontroller, DC motors with control circuits, optical sensors to measure the reflectivity of the surface on which it is standing, a three-axis gyroscope, an accelerometer, and a photoresistor. The entire block structure is shown in Fig.4.

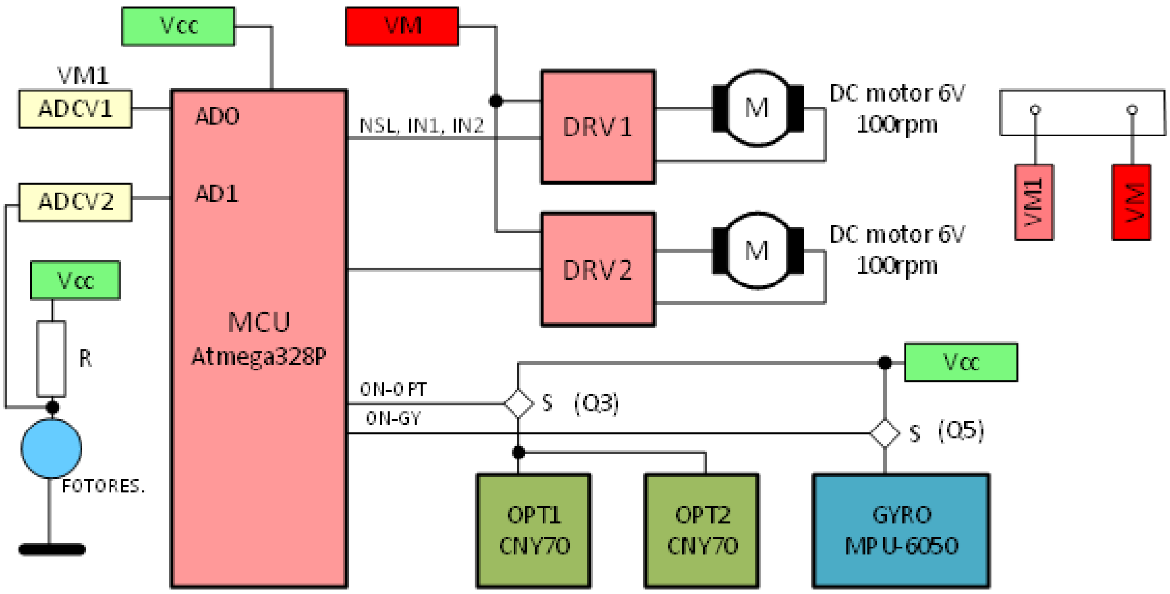

Fig.4 Block diagram of Solar Car control parts

To develop the Solar Car software, the following technical resources are required:

- Solar Car,
- Computer (PC, Notebook, etc.) with two free USB ports,
- USBASP programmer,
- USB/UART converter module.

IV. Typical Task

The students are provided with complete technical documentation about the car so that they can solve the problems given. One typical task is the task of tracing a black line on a white background. The line is approximately 2 meters long and the car must cross it in the shortest possible time. The power of the solar panel is not large enough to move the car based on the power of the solar panel alone. The energy needs to be stored in a supercapacitor ($E_{max} = \frac{1}{2}CU^2$). In our case, a supercapacitor with a capacity of 1 F is used to store energy. Its maximum stored energy is 18 J at 6 V. This is not enough energy to travel the entire specified path. It is necessary to stop and wait for the supercapacitor to recharge. The voltage on the supercapacitor (VM in Figure 3) can be measured using the MCU. It is necessary to decide at what voltage it is appropriate to stop the motion, recharge the supercapacitor and start moving again. Other questions to be answered are: When is it appropriate to turn in the direction of maximum illumination when charging? Should the point of maximum solar cell power be considered? How to track the line using optical sensors? Is it worth turning them off and on? What MCU clock frequency to choose? Which MCU peripherals should be switched off and which not? Is it also worth using gyro information or leaving it off?

These and many other questions need to be answered during application development. Knowledge of electronics, programming, physics and the ability to use them effectively are required to solve the above task. Usually, the students' work ends with a final competition, during which there are always problems that have been forgotten in the course of the solution. But also many new possibilities for solving the problems. Figure 5 illustrates the progress of the parallel slalom competition.

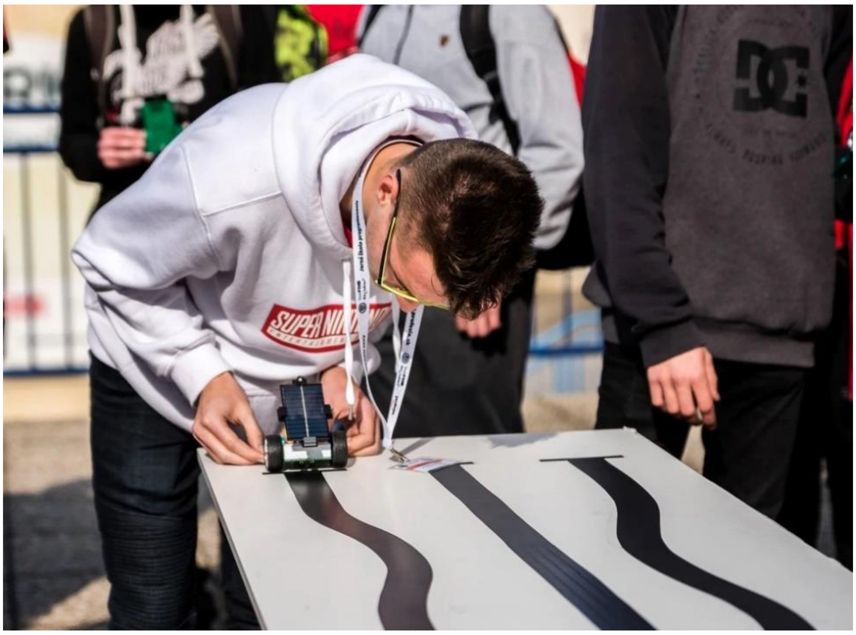

Figure 5 Solar Car, parallel slalom

V. Conclusion

The primary objective of the Solar Car project was to increase the interest of students in studying the technical fields of ICT, specifically Computer Engineering. The students were to learn about the development of a programmable MCU-based device in a fun way. It was not the development of a professional device. We focused on such a way of solving the task to make it accessible to a wide group of high school students without much professional knowledge. Obviously, the choice of a very simple ATmega328 microcontroller and the C/C++

programming language was also subordinated to this intention. Parallel to the Solar Car project, several projects of a similar nature have been developed (Rail Gun project, WiFi Boat and others). In conclusion, we can say that the interest of students in taking a one-week course resulting in a "live" product is very high.

ACKNOWLEDGMENT

This article was created in the framework of the National project „IT Academy – Education for the 21st Century“, which is supported by the European Social Fund and the European Regional Development Fund in the framework of the Operational Programme Human Resources, ITMS code of the project: 312011F057.

REFERENCES

[1] J. Malmodin, N. Lövehagen, P. Bergmark, and D. Lundén, "ICT sector electricity consumption and greenhouse gas emissions – 2020 outcome," *Telecommunications Policy*, vol. 48, no. 3, Apr. 2024.

[2] P. Valerio, "Energy efficiency is crucial for the ICT infrastructure," *EE Times*, Apr. 24, 2023. [Online]. Available: https://www.eetimes.com/energy-efficiency-is-crucial-for-the-ict-infrastructure/. [Accessed: 30-Nov -2024].

[3] H. Ritchie, "What's the impact of artificial intelligence on energy demand?" *Sustainability by Numbers*, Nov. 18, 2024. [Online]. Available: https://www.sustainabilitybynumbers.com/p/. [Accessed: 30-Nov -2024].

[4] "What's the difference between a primary and secondary battery?" *PK Cell Power*, Apr. 26, 2024. [Online]. Available: https://www.pkcellpower.com/news/whats-the-difference-between-a-primary-and-secondary-battery/. [Accessed: 30-Nov -2024].

[5] "Will secondary batteries replace primaries?" *Battery University*. [Online]. Available: https://batteryuniversity.com/article/will-secondary-batteries-replace-primaries. [Accessed: 30-Nov -2024].

[6] U. Tiwari, "What is the difference between supercapacitors and batteries?" *Malvern Panalytical*, May 7, 2024. [Online]. Available: https://www.malvernpanalytical.com/en/learn/knowledge-center/insights/what-is-the-difference-between-supercapacitors-and-batteries. [Accessed: 30-Nov -2024].

Enhancing Biosignal Data Analysis with LSL and BioLab

Ján Stehlík, Michal Kubaščík, Peter Šarafín

Abstract— Efficient collection and analysis of biological signals are essential for progress in neuroscience, physiology, and related fields. These capabilities address the increasing complexity of modern experimental setups, allowing researchers to focus on insights rather than technical challenges. The Lab Streaming Layer provides a comprehensive system for managing time-series data, offering solutions for networking, precise time synchronization, and real-time access across devices such as electroencephalography and eye-tracking tools. Complementing this, the Biosignals Laboratory simplifies the process of streaming and analyzing signals online through configurable scripts. Together, these tools streamline workflows, enabling seamless real-time insights and fostering innovation in the study of biological signals. This paper examines their capabilities, practical applications, and future potential.

Keywords— Biological signals, electroencephalography, data synchronization, signal processing.

I. INTRODUCTION

In modern research, the ability to seamlessly collect, synchronize, and analyze biosignal data is critical for advancing our understanding of human physiology and behavior. The Lab Streaming Layer (LSL) provides a robust framework for unified data collection in experimental settings, enabling real-time access, time synchronization, and centralized recording[1]. This open-source system supports diverse devices, from EEG and fNIRS to eye-tracking equipment, and integrates seamlessly across multiple programming languages, making it a versatile tool for researchers across disciplines.

Complementing LSL is the Biosignals Laboratory (BioLab), a project designed to simplify signal streaming and data analysis. By leveraging configurable scripts, Biolab streamlines the creation of data streams, providing users with accessible tools to visualize, analyze, and process incoming data in real-time. The integration of BioLab with LSL offers unparalleled flexibility, allowing researchers to connect to and manage biosignal streams effortlessly.

This article delves into the key features of LSL and Biolab, provides practical examples of their applications, and explores potential future developments that could further transform biosignal research. Whether you are an academic, a developer, or a professional in the field, these tools present exciting opportunities to enhance data-driven discoveries and innovation.

II. LAB STREAMING LAYER

The Lab Streaming Layer (LSL) is a comprehensive framework designed to unify the collection and management of measurement time series in research experiments. Its robust system facilitates the seamless integration of various data sources, addressing critical aspects such as networking, precise time synchronization, near-real-time data access, and optional centralized collection. By resolving common data synchronization and integration challenges, LSL significantly improves the efficiency of experimental workflows, particularly in multi-device environments. This centralized capability allows for efficient viewing, recording, and archiving of data directly onto a disk, making LSL an essential tool in research workflows[2].

Ján Stehlík, University of Zilina, Zilina, Slovakia (e-mail: stehlik16@stud.uniza.sk)
Michal Kubaščík, University of Zilina, Zilina, Slovakia (e-mail: michal.kubascik@fri.uniza.sk)
Peter Šarafín, University of Zilina, Zilina, Slovakia (e-mail: peter.sarafin@fri.uniza.sk)

This versatility makes LSL invaluable for a range of applications, from monitoring neural activity to studying eye movements, enhancing both research accuracy and efficiency. To visualize its functionality, imagine a network with two primary applications: an outlet and an inlet. The outlet serves as the source of streaming data, broadcasting its availability to the network. The inlet, acting as the receiver, identifies and connects to the outlet. Once connected, the outlet buffers data and transmits it upon the inlet's request. This architecture ensures a smooth flow of data between connected devices, even in demanding research scenarios.

What makes LSL particularly versatile is its wide compatibility with numerous programming languages and a diverse range of supported devices. These include cutting-edge tools like EEG systems, functional near-infrared spectroscopy (fNIRS), and eye-tracking devices. This broad support allows researchers across multiple disciplines to adopt LSL in their experimental setups, simplifying the challenges of integrating heterogeneous data sources into a cohesive system[3][4].

By leveraging LSL, researchers can focus on data-driven insights rather than the technical intricacies of data collection and synchronization, paving the way for innovative breakthroughs in neuroscience, physiology, and other fields [5].

III. BioLab

The Biosignals Laboratory (Biolab) is an innovative project designed to facilitate the streaming of signals and data for real-time online analysis. By employing configuration files and scripts, Biolab enables users to efficiently create and manage stream outlets, simplifying the process of collecting and analyzing biosignal data. This structured approach allows researchers to focus on data interpretation and application rather than dealing with complex setup procedures.

A. Examples

Biolab examples showcase practical implementations of LSL and Biolab, focusing on how to establish inlets and efficiently extract and process received data streams. There are currently 3 example programs, which are stream search, select stream and plot data. Each example demonstrates a specific aspect of these tools, making it easier for users to understand and apply their functionalities in real-world scenarios.

1) Stream search

This program allows the user to search for available streams. Upon running the program, the user is asked to type into the terminal the type of stream that they wish to search for. If left empty, the program will search for all available streams, otherwise it will search for streams of that type.

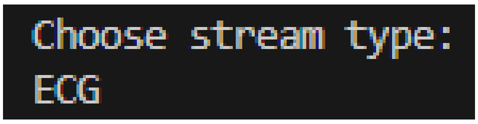

Fig. 1 Example of choosing stream type

If any number of streams are found, their name, type, channel count and user id (UID) will be written on the terminal. If none are found, the message “No streams were found” will be printed on the terminal.

```
Looking for EEG streams...
2024-11-24 15:53:22.435 (   4.539s) [        5F5902C]      netinterfaces.cpp:36    INFO| netif '{A81891A8-4A91-4F
07-8D4B-90AFE7B4678A}' (status: 1, multicast: 1
2024-11-24 15:53:22.435 (   4.539s) [        5F5902C]      netinterfaces.cpp:36    INFO| netif '{3285BD52-5F4F-4F
65-AB66-3B82E8A78F64}' (status: 2, multicast: 1
2024-11-24 15:53:22.435 (   4.540s) [        5F5902C]      netinterfaces.cpp:36    INFO| netif '{8CA27D4A-24D7-40
48-9D51-9D6F5774539E}' (status: 2, multicast: 1
19-8342-F3E4A342BC4B}' (status: 2, multicast: 1
2024-11-24 15:53:22.436 (   4.540s) [        5F5902C]      netinterfaces.cpp:36    INFO| netif '{85C9A568-0283-49
42-B890-F717008A29DF}' (status: 2, multicast: 1
2024-11-24 15:53:22.436 (   4.540s) [        5F5902C]      netinterfaces.cpp:36    INFO| netif '{1AA6237C-273B-11
EC-B1C8-806E6F6E6963}' (status: 1, multicast: 1
2024-11-24 15:53:22.436 (   4.540s) [        5F5902C]      netinterfaces.cpp:58    INFO|       IPv6 ifindex 1
2024-11-24 15:53:22.436 (   4.540s) [        5F5902C]        api_config.cpp:270    INFO| Loaded default config
1 were found:
BioSemi   EEG   8   f27926a2-6814-40e9-96be-3af52b6cfc63
```

Fig. 2 Console output of found stream

2) Select stream

This program allows the user to connect to a stream by their name, user id and type. At first, the program asks the user to type the name, UID and type into the terminal. The program then attempts to find the streams based on the user’s input.

```
Type the name of the stream:
BioSemi
Type the uid of the stream:
EEG
Type the type of the stream:
f27926a2-6814-40e9-96be-3af52b6cfc63
Finding stream...
```

Fig. 3 Example of user input for select stream

If no such streams are found, a message will be printed on the terminal. If one stream is found, the program will immediately connect to the stream and a confirmation message will be printed on the terminal. If multiple streams of such type are found, the user is asked to select the stream they wish to connect to, after which the program connects to the selected stream.

```
Finding stream...
2024-11-24 16:13:45.820 (  28.195s) [        4A20D6B2]      netinterfaces.cpp:36    INFO|
2024-11-24 16:13:45.821 (  28.195s) [        4A20D6B2]      netinterfaces.cpp:36    INFO|
2024-11-24 16:13:45.821 (  28.195s) [        4A20D6B2]      netinterfaces.cpp:36    INFO|
2024-11-24 16:13:45.821 (  28.195s) [        4A20D6B2]      netinterfaces.cpp:36    INFO|
2024-11-24 16:13:45.821 (  28.195s) [        4A20D6B2]      netinterfaces.cpp:36    INFO|
2024-11-24 16:13:45.821 (  28.195s) [        4A20D6B2]      netinterfaces.cpp:36    INFO|
2024-11-24 16:13:45.821 (  28.195s) [        4A20D6B2]      netinterfaces.cpp:58    INFO|
2024-11-24 16:13:45.821 (  28.195s) [        4A20D6B2]        api_config.cpp:270    INFO|
2024-11-24 16:13:46.323 (  28.697s) [        4A20D6B2]            common.cpp:65     INFO|
Connected to stream
```

Fig. 4 Example output of a successful connection to a stream

3) Plot data

This program allows the user to connect to a stream and plots raw data from the stream. We have chosen to use the pyqtgraph graphics library to plot the data.

The program first searches for available streams. If none are found, a message will be printed. Otherwise, the user is asked to choose the stream to plot.

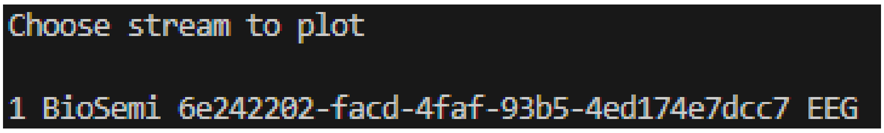

Fig. 5 Example output of available streams

Afterwards, the created inlet pulls data in chunks and plots the data onto a graph. Data from each channel is plotted on a separate curve. Each curve has a unique color (if the channel count is 8 or less).

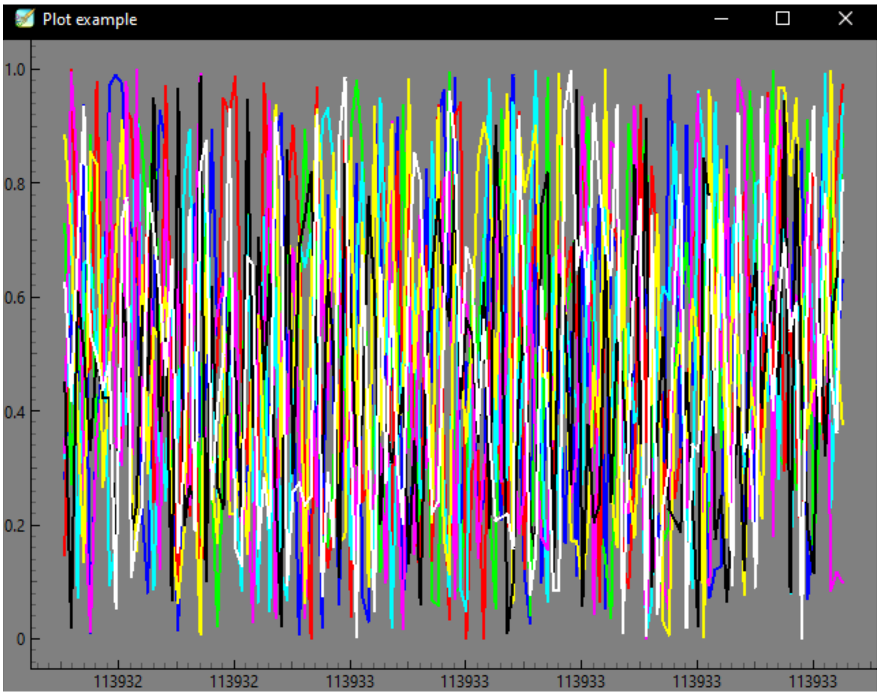

Fig. 6 Graph output for stream data

IV. Future expansion of examples

Future expansion plans include enhancing data visualization capabilities by allowing users to selectively display specific streams or transitioning to a stand-alone online viewer for more flexible and intuitive data analysis. Additionally, there will be developed new example focused on the filtration and analysis of biosignal data, further broadening the range of tools available for advanced data processing and insights. These updates aim to improve user experience, increase analytical flexibility, and support more sophisticated data handling in complex research environments[6].

V. Conclusion

The Lab Streaming Layer and Biosignals Laboratory provide powerful and versatile solutions for the collection, synchronization, and analysis of biosignal data. These tools streamline workflows by offering real-time data access, seamless integration with various devices, and simplified data management through configurable scripts. By alleviating the technical burdens of data management, LSL and BioLab empower researchers to delve deeper into analytical exploration, driving innovation and advancing discoveries in neuroscience and beyond. As these technologies evolve, they hold significant potential for further improving the efficiency and flexibility of biosignal research, paving the way for new discoveries and advancements in scientific exploration[1][5][6].

REFERENCES

[1] C. Kothe, D. Medine, C. Boulay, M. Grivich, and T. Stenner, "Introduction — Labstreaminglayer 1.13 documentation," 2019. [Online]. Available: https://labstreaminglayer.readthedocs.io/info/intro.html. [Accessed: Nov. 24, 2024].

[2] C. Kothe, D. Medine, C. Boulay, M. Grivich, and T. Stenner, "User's Guide — Labstreaminglayer 1.13 documentation," 2019. [Online]. Available: https://labstreaminglayer.readthedocs.io/info/user_guide.html. [Accessed: Nov. 24, 2024].

[3] C. Kothe, D. Medine, C. Boulay, M. Grivich, and T. Stenner, "Supported Devices and Tools — Labstreaminglayer 1.13 documentation," 2019. [Online]. Available: https://labstreaminglayer.readthedocs.io/info/supported_devices.html. [Accessed: Nov. 24, 2024].

[4] "Tips and tricks for using Lab Streaming Layer (LSL)." [Online]. Available: https://www.brainproducts.com/support-resources/tips-and-tricks-for-lsl/. [Accessed: Dec. 1, 2024].

[5] C. Kothe, S. Y. Shirazi, T. Stenner, D. Medine, C. Boulay, M. Grivich, T. Mullen, A. Delorme, and S. Makeig, "The Lab Streaming Layer for synchronized multimodal recording," *bioRxiv*, 2024. [Online]. Available: https://doi.org/10.1101/2024.02.13.580071. [Accessed: Dec. 1, 2024].

[6] Q. Wang, Q. Zhang, W. Sun, C. Boulay, K. Kim, and R. L. Barmaki, "A scoping review of the use of Lab Streaming Layer framework in virtual and augmented reality research," *Virtual Reality*, 2023. [Online]. Available: https://doi.org/10.1007/s10055-023-00799-8. [Accessed: Dec. 1, 2024].

Autommated Terrarium Implementation

Tomáš Bača, Ján Šumský, Michal Kubaščík, Peter Šarafín

***Abstract*—** The automated terrariums represent an interesting application for automatization. The goal of the work presented in this article was the development of an automated terrarium that could control the temperature and humidity inside the terrarium. The automation also consisted of automatic watering of the animals inside the terrarium. The work was later on improved by the addition of the Wi-Fi module and the creation of a web page through which the user could set the required and monitor the current temperature and humidity.

***Keywords*—** automatization, atmega328P, electromagnetic valve, heating resistors, LCD display, bang-bang regulation, PID regulation

I. INTRODUCTION

The goal of this article is to present the result of the work which was focused on the creation of such an automated terrarium. The automatization consisted of the automatic temperature and humidity control system. And the automatic watering of the animals living in the terrarium. The work was extended by the addition of the wireless communication module, which was running a web page through which the user could interact with the automated terrarium.

II. DEVELOPMENT OF AUTOMATED TERRARIUM

This paper is focused on the development of small automated terrariums that used as box and aquariums. The main goals from the point of view of automatization were the automatic humidity and temperature control to the values set by the user, the automatic watering of the animal inside of the terrarium and the creation of a simple user interface with the use of buttons, rotary encoders and an LED display capable of showing to the user 32 symbols at the same time.

In this work was also designed the printed circuit board (PCB) at which were placed all the SMD components and to which were connected by wires certain sensors and action elements.

Basic functionality was extended by connecting the originally used printed circuit board with the microcontroller ATMega328P to a module containing the microcontroller ESP32-S1 which supported wireless communication. And creating a web page through which the temperature and humidity could be set and controlled. This web page served as a graphical user interface and it turned the developed automated terrarium into an IoT application.

A. Sensors

In the automated terrarium development two different sensors were used.

The first sensor was the DHT11 [1], this sensor measured the temperature and humidity inside of the terrarium. This sensor was communicating with the microcontroller ATMega328P through a proprietary communication protocol.

The second sensor was measuring the water level, this sensor was placed inside of the bowl with water from which the animal was being watered. The sensor had an analog output which was processed by the analog-to-digital converter inside of the microcontroller ATMega328P used in this application.

Tomáš Bača, University of Žilina, Slovak Republic (e-mail: tomas.baca@fri.uniza.sk)
Ján Šumský, University of Žilina, Slovak Republic (e-mail: jan.sumsky@fri.uniza.sk)
Michal Kubaščík, University of Žilina, Slovak Republic (e-mail: michal.kubascik@fri.uniza.sk)
Peter Šarafín, University of Žilina, Slovak Republic (e-mail: peter.sarafin@fri.uniza.sk)

B. Action elements

In the automated terrarium developed during the bachelor theses were used five types of action elements.

The first action element was two electromagnetic valves. These valves were used in the vertical position and they were fixed to the two walls of the terrarium. Both of these valves had on their upper sides bottles with water which served as the water reservoir. Underneath these valves were placed two bowls into which the water could flow. One of the bowls was used for watering the animal and the other bowl was used for increasing the humidity in the terrarium.

The second action element was two heating resistors [2]. The first heating resistor was used to control the temperature in the terrarium during its operation it heated the air inside of the terrarium. The second heating resistor was placed under one of the bowls with the water. When this second heating resistor is turned on it will start heating the water. The heated water will start to evaporate and as a result of this evaporation of the water the humidity in the terrarium will be increased.

Both the electromagnetic valves and the heating resistors were using as a power supply 12V voltage source. All four of these elements were controlled by the output pins. The microcontroller ATMega328P had on its output pins when set to logic one voltage 5V. Because of this, the N MOSFETs were used as switches. When the output pin is set to logic one the N MOSFET will turn on the power to the electromagnetic valve or a heating resistor will be supplied. And when the output pin is set to logic zero the N MOSFET will be turned off and no power is being supplied.

The third action element was the LCD display. During the normal operation of the terrarium on this display were shown the last measured values of the temperature and humidity. When the user was setting the wanted temperature and the humidity in the terrarium these values were also shown on this LCD display. The LCD display was capable of displaying the letters of the Latin alphabet, the number and certain special symbols. The LCD display contained two lines, and each of them was capable of displaying 16 symbols, therefore the total number of symbols that could be shown at the same time was 32. This display was communicating with the microcontroller ATMega328P through the communication interface I2C.

The fourth action element was the electromagnetic buzzer. This buzzer was controlled by the PWM pin of the microcontroller ATMega328P. This buzzer was used as an audible alarm in error situations. One example of an error situation was when sensors measured higher values of temperature or humidity than the values set by the user. This situation could occur naturally by the influence of the temperature and humidity of the surrounding environment in which the automatic terrarium was placed. Or by some error in the control or operation of the heating and moisturizing elements.

The fifth action element was the RGB LED diode, on this diode were shown different colours based on the specific actions that the system was performing at that time. The RGB LED diode was controlled by the three pins of the microcontroller ATMega328P.

C. Control elements

In the automated terrarium development two different control elements were used.

The first control element was the rotary encoder. With this control element, the user could set the required value of temperature and humidity in the terrarium. This rotary encoder was sending data into the two input pins of the microcontroller ATMega328P.

The second control element was two buttons connected to two input pins of the microcontroller ATMega328P. After the user pressed the first button he went into a mode in which he could change the required values of the temperature and humidity by the rotary encoder, in this mode were also shown on the LCD display the currently set values of temperature and humidity. The second button was not used in the final version of the application, it was used just during the testing of the application.

D. Microcontroller

In the automated terrarium used the microcontroller ATMega328P [3] as a control unit. It is a low-power AVR 8-bit microcontroller with advanced RISC architecture. The microcontroller was programmed in the programming language C++.

This microcontroller has 32 eight-bit universal registers. 32 KB of programmable flash memory, 1 KB of EEPROM memory and 2 KB of internal SRAM memory.

This microcontroller was chosen because of its low power consumption and easy internal architecture that allowed it to be programmed through the registers without bigger complications.

The microcontroller was using as the clock signal its internal RC oscillator which is working at the frequency of 1 MHz.

E. Control algorithms

In the automated terrarium three different control algorithms was implemented.

The first control algorithm was responsible for sustaining certain levels of water in the bowl used for watering the animal. If the sensor in the bowl detected water level under a certain minimal threshold, the electromagnetic valve on top of the bowl would open for a short time and let a small amount of water flow into the bowl. This was repeated until the sensor detected a water level above the maximal threshold. If this process was repeated 10 times but the water level in the bowl didn't increase the system would throw out an error and start the audible alarm to get the attention of the user.

The second control algorithm was responsible for sustaining the required temperature in the terrarium. If the temperature sensor detects a lower temperature then the heating resistor will be turned on. During experiments were used two types of control algorithms for determining the intensity of the heat supplied by the heating resistor.

The third control algorithm was responsible for sustaining the required humidity in the terrarium. If the humidity sensor detected a lower humidity then the electromagnetic valve on top of the bowl would open for a short time and let a small amount of water flow into the bowl. In the next step, the heating resistor under this bowl was turned on causing the water to evaporate and as a result, increase the humidity in the terrarium.

In the end, both the temperature and humidity were controlled by the bang-bang regulation. The bang-bang regulation doesn't take into account the size of the gradient between the required and actual temperature or humidity. If the system detects a lower actual value than the predefined it just simply activates the action element in our case the heating resistors for a predefined amount of time. After this time passes the sensor will again take a measurement and if the actual value is still lower than the required the action element will get again activated for the predefined time.

The bang-bang regulation represents a very simple form of regulation, in most cases even this simple regulation can, in the end, achieve the required value of the affected parameter, however, the bang-bang regulators can take a long time before they will achieve this required value.

This regulation could be improved by the use of the P, PI or PID regulators [4] which take into account the size of the gradient between the required and actual temperature or humidity. The P, PI and PID regulators will be explained in the temperature control.

The final intensity of the heat supplied by the heating resistor (the duty cycle of the used PWM signal) is determined by the final value from the output of the P, PI or PID controller.

In the simplest control algorithm, the intensity of the heating resistor was proportional to the thermal gradient between the actual and required temperature multiplied by a constant. This is called simple proportional control and the used type of controller is called the P controller.

The time required for heating up the terrarium from room temperature to the required temperature could be improved by the use of the second type of heat control algorithm, the proportional integral control and this type of controller is called the PI controller.

The integral components sum the previously measured thermal gradients both positive and negative. The proportional component just takes the current thermal gradient.

Both the proportional and integral elements are then multiplied by different constants. These two elements after the multiplication are summed together and we get the final value from the output of the PI controller.

The final value from the output of the PI controller depends on the chosen constants with which are multiplied the proportional and integral elements.

However, if the constant for the integral element is chosen too high then the overshoot will occur. The overshoot is basically an output temperature that is higher than the required temperature.

The regulation could be further improved by the use of a PID regulator which has an additional derivation element. The final value from the output of the PID controller is calculated as the sum of the three elements multiplied by three different constants.

The derivation element is calculated as the difference between the two successive measured values. The derivation element could help improve the resistance of the controller system (temperature in the terrarium) to sudden external changes in temperature.

The problem with the PI regulation is that if a sudden change in the external temperature occurs such as when someone opens a window close to the terrarium in the middle of the winter, the temperature in the terrarium will quickly drop down. The proportional and the integral elements are not capable of quickly responding to this quick change in the temperature and it would take them some time to increase the temperature to the desired temperature.

However, the derivation element will detect this sudden change in temperature between the two successive measured values. Then it will quickly increase the final value from the output of the PI controller. This will result in a quick increase in the intensity of the temperature of the heating resistor which will counteract the lowering of temperature caused by the external factors.

However, just like with the integral element if the constant for the derivation element is chosen too high then the overshoot will occur.

The other problem connected with the P, PI and PID regulations in this application is the propagation delay caused by the fact that the heating resistor is placed on one side of the terrarium and the temperature sensor is placed on the other side of the terrarium, therefore we have to use in the calculations also the fact that even though the sensor is measuring smaller temperature than the required, the temperature on the side of the terrarium where the heating element is located could be already higher than the required temperature, and if we will don't decrease the intensity of the heating element before the measured temperature equal the required temperature we could actually create a big overshoot.

III. Results of the performed experiments

The experiments were performed with the bang-bang regulation. Throughout the experiments, different times during which the action element (heating resistor) was active were tested.

Later on through the experiments, the bang-bang regulation was adjusted by monitoring the current temperature/humidity during the time that the active element was active and the termination of the heating process ahead of the planned schedule if the required temperature or humidity was achieved before the heating cycle ended.

The last adjustment to the bang-bang regulation was the decrease in the temperature and humidity at which the regulator stopped powering the heating element. This was done since this system has in it the propagation delay.

During the experiments, the system was capable of achieving the required temperature and humidity with this adjusted bang-bang regulation algorithm.

In the graphs showing the result of the final experiment the required temperature was 26O C and the required humidity was 48%.

Through the experiment, the humidity of the air in the terrarium was artificially increased by the vaporizer which blew water steam into the terrarium and thus increased the humidity. From the results can be seen that the regulation was capable of dealing with this problem and achieved the desired humidity.

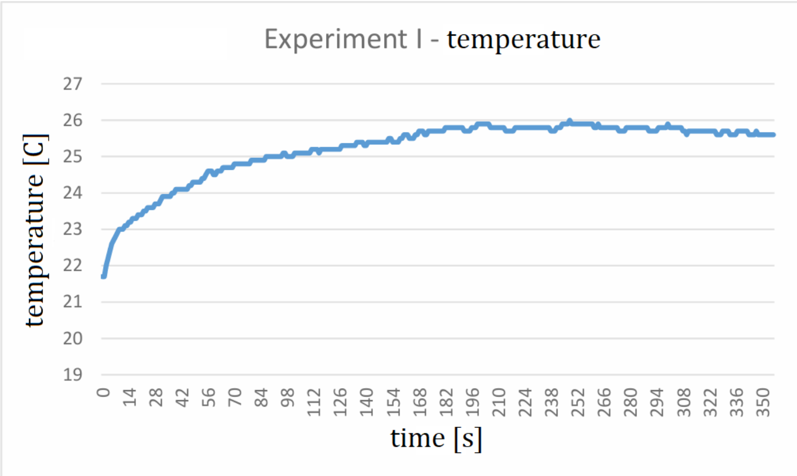

Figure 1. Experiment graph temperature

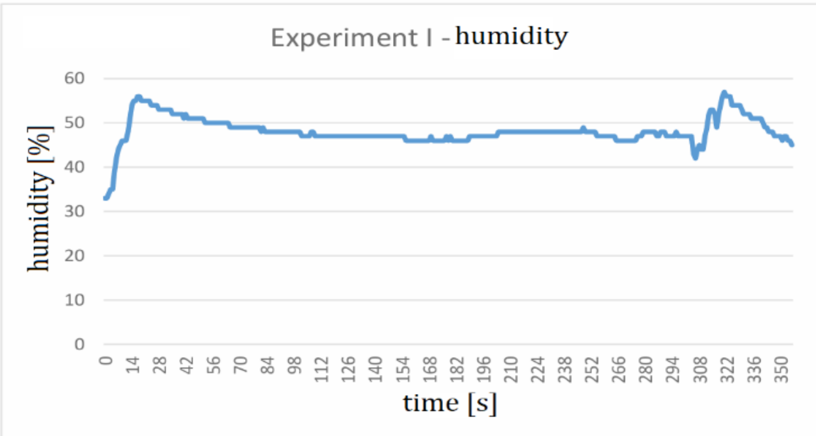

Figure 2. Experiment graph humidity

References

[1] "DHT11," *ElectronicWings*. [Online]. Available: https://www.electronicwings.com/sensors-modules/dht11. [Accessed: Dec. 6, 2024].

[2] "Heater resistor applications," *EE Power*. [Online]. Available: https://eepower.com/resistor-guide/resistor-applications/heater-resistor/#. [Accessed: Dec. 6, 2024].

[3] "ATmega328P datasheet," *Microchip Technology*, 2019. [Online]. Available: https://ww1.microchip.com/downloads/en/DeviceDoc/Atmel-7810-Automotive-Microcontrollers-ATmega328P_Datasheet.pdf. [Accessed: Dec. 6, 2024].
[4] M. R. James, "Design and implementation of proportional-integral-derivative (PID) controllers," *IEEE Transactions on Control Systems Technology*, vol. 16, no. 6, pp. 1375–1381, Nov. 2008. doi: 10.1109/TCST.2008.2000560.

ESP32 - Based Pulse Oximeter

Matúš Dikoš, Michal Kubaščík, Veronika Olešnaníková, Peter Ševčík

***Abstract*—**The project involved developing a device for monitoring pulse and blood oxygen levels using an ESP32 microcontroller and various sensors. The device measures these physiological parameters and transmits the collected data via Wi-Fi to a mobile device. This straightforward solution demonstrates the practical application of available technologies for creating a simple health-monitoring tool.

***Keywords*—**blood oxygen levels, ESP32, health monitoring, microcontroller-based systems, wireless data transmission

I. INTRODUCTION

The project aimed to develop a simple, compact and cost-effective device for monitoring pulse and blood oxygen levels. The design prioritized portability and ease of use, resulting in a small, wireless solution built using the ESP32-S2 Mini microcontroller and the MAX30102 sensor. This combination enabled real-time data collection and transmission via Wi-Fi to a mobile device, providing users with immediate access to health metrics in an intuitive way.

The project illustrates the versatility of modern microcontrollers and sensors in addressing everyday health-monitoring needs. By leveraging accessible and cost-effective components, the device demonstrates how basic biomedical measurements can be integrated into a lightweight and user-friendly tool. The ability to operate without reliance on external networks further enhances its functionality, making it suitable for a variety of applications, such as personal health tracking, educational demonstrations, or prototyping for more advanced medical devices.

This approach highlights the potential for such technologies to make health monitoring more accessible and practical in various contexts, from individual use at home to projects within academic settings. The simplicity of the design ensures that the device remains functional while still being easy to build, modify, and expand for future needs.

II. PURPOSE OF THE DEVICE

The design prioritized portability and ease of use, resulting in a small, wireless solution built using the ESP32-S2 Mini microcontroller and the MAX30102 sensor. This combination enabled real-time data collection and transmission via Wi-Fi to a mobile device, providing users with immediate access to health metrics in an intuitive way.

The project illustrates the versatility of modern microcontrollers and sensors in addressing everyday health-monitoring needs. By leveraging accessible and cost-effective components, the device demonstrates how basic biomedical measurements can be integrated into a lightweight and user-friendly tool. The ability to operate without reliance on external networks further enhances its functionality, making it suitable for a variety of applications, such as personal health tracking, educational demonstrations, or prototyping for more advanced medical devices.

This approach highlights the potential for such technologies to make health monitoring more

Matúš Dikoš, University of Zilina, Zilina, Slovakia (e-mail: dikos@stud.uniza.sk)
Michal Kubaščík, University of Zilina, Zilina, Slovakia (e-mail: michal.kubascik@fri.uniza.sk)
Veronika Olešnaníková, University of Zilina, Zilina, Slovakia (e-mail: veronika.olesnanikova@fri.uniza.sk)
Peter Ševčík, University of Zilina, Zilina, Slovakia (e-mail: peter.sevcik@fri.uniza.sk)

accessible and practical in various contexts, from individual use at home to projects within academic settings. The simplicity of the design ensures that the device remains functional while still being easy to build, modify, and expand for future needs.

III. BUILDING AND IMPLEMENTING THE DEVICE

A. ESP32-S2 MINI

For this implementation, we used the ESP32-S2 Mini microcontroller as the central unit for both data collection and communication. The ESP32-S2 Mini is powered by a 32-bit single-core processor running at up to 240 MHz, and features integrated Wi-Fi capabilities, which are crucial for wireless data transmission. With 4 MB of flash memory, the microcontroller provides sufficient storage for handling and processing sensor data in real-time.

In this project, the ESP32-S2 Mini was responsible not only for transmitting pulse and blood oxygen level data over Wi-Fi but also for collecting and evaluating the data from the MAX30102 sensor. The microcontroller processes the raw sensor readings, applies necessary calculations, and prepares the data for transmission. This dual functionality - acting as both a data acquisition system and a communication hub-enabled the development of an efficient and compact health-monitoring device. The low power consumption and small form factor of the ESP32-S2 Mini made it an ideal choice for the portable device, allowing it to seamlessly collect, process, and transmit data in real-time.

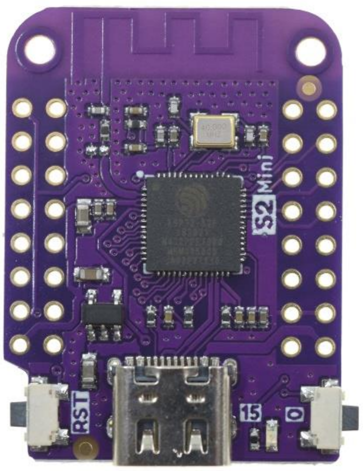

Fig. 1 Development board ESP32-S2FN4R2 developed by Wemos.

B. MAX30102

The sensor is made up of two light-emitting diodes (LEDs), one emitting monochromatic red light at a wavelength of 660 nm and the other emitting infrared light at 940 nm. These specific wavelengths are selected because oxygenated and deoxygenated hemoglobin have distinct absorption characteristics at these wavelengths. As demonstrated in the graph below, oxygenated hemoglobin (HbO2) and deoxygenated hemoglobin (Hb) exhibit noticeable differences in their absorption of red and infrared light.

The sensor consists of two main components: the emitting diodes and a photodetector. The LEDs emit light, which passes through the finger when placed steadily on the sensor. Oxygenated blood absorbs some of the light, while the rest is reflected through the finger and detected by the photodetector. The photodetector captures this reflected light, and the data is then processed and read by a microcontroller to determine the blood oxygen levels.

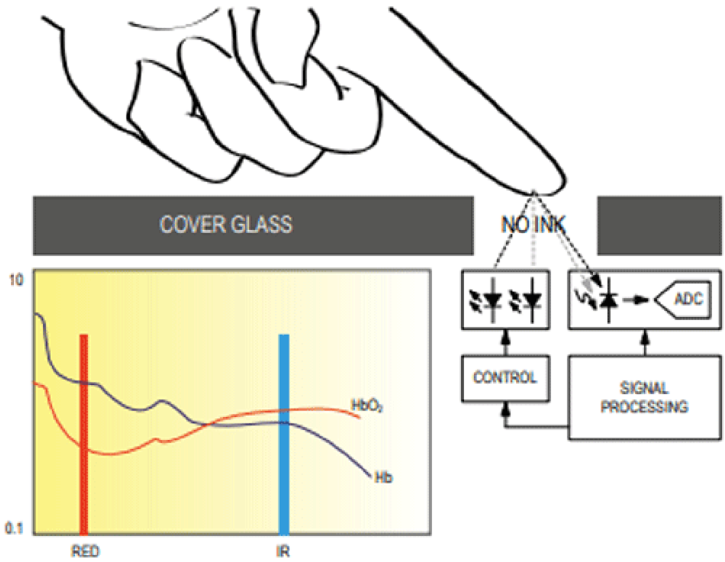

Fig. 2 MAX30102 sensor for pulse and blood oxygen level monitoring

C. Communication

In principle, the project aimed to develop a simple and compact device for monitoring pulse and blood oxygen levels. The design prioritized portability and ease of use, resulting in a small, wireless solution built using the ESP32-S2 Mini microcontroller and the MAX30102 sensor. This combination enabled real-time data collection and transmission via Wi-Fi to a mobile device, providing users with immediate access to health metrics in an intuitive way.

The project illustrates the versatility of modern microcontrollers and sensors in addressing everyday health-monitoring needs. By leveraging accessible and cost-effective components, the device demonstrates how basic biomedical measurements can be integrated into a lightweight and user-friendly tool. The ability to operate without reliance on external networks further enhances its functionality, making it suitable for a variety of applications, such as personal health tracking, educational demonstrations, or prototyping for more advanced medical devices.

This approach highlights the potential for such technologies to make health monitoring more accessible and practical in various contexts, from individual use at home to projects within academic settings. The simplicity of the design ensures that the device remains functional while still being easy to build, modify, and expand for future needs.

D. Heart rate

To calculate the heart rate from the sensor data, the code first reads the infrared (IR) value from the MAX30102 sensor. It checks for a beat by using the checkForBeat() function, which detects the pulse. When a beat is detected, the time difference between the current reading and the last beat (delta) is calculated. This time difference is then used to calculate the beats per minute (BPM).

The calculated BPM is checked to ensure it falls within a valid range, typically between 40 and 220. If the BPM is valid, it is stored in an array for averaging over multiple readings. The average heart rate is then calculated by summing the most recent readings and dividing by the total number of readings to smooth out any fluctuations in the data.

E. Blood oxygen

The MAX30102 sensor is also capable of measuring blood oxygen levels (SpO2). Like the heart rate calculation, the sensor uses red and infrared LEDs to illuminate the blood vessels, and the reflection of this light is measured to estimate the amount of oxygen in the blood. The sensor calculates the ratio of the absorption of red and infrared light to determine the oxygen saturation level.

In this implementation, the sensor continuously collects this data, and the values are processed to calculate the SpO2 percentage. The code uses the MAX30102's built-in functions to retrieve the necessary raw data for this calculation. Once the values are processed, they are displayed on the OLED screen, alongside the heart rate, providing a simple yet effective way to monitor both metrics in real-time. The sensor's ability to manage both pulse and blood oxygen measurements makes it ideal for creating a compact, multi-functional health-monitoring device.

IV. FUTURE EXPECTATIONS

In future research will be device improved by external battery management system and ESP32-C3 development board, bringing up optimization size, power consumption and performance of device. Consequently, data will be transmitted over Wi-Fi to cloud storage with time series database, or via Bluetooth Low Energy to mobile application and further stored in cloud storage. Harvested data will be used for advanced medical analysis and health issues prediction, health management. The concept of the new device and health system is described in Fig. 3. Main purpose of the device is to match Health 4.0 standards.

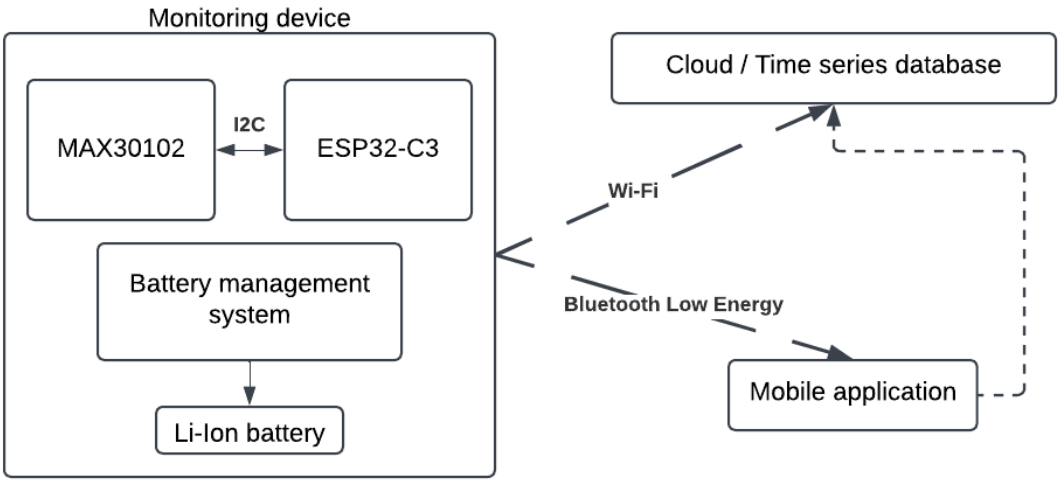

Fig. 3 Improved device design and health monitoring system

V. CONCLUSION

The creation of a compact, wireless health monitoring device capable of measuring heart rate and blood oxygen levels demonstrates the practical application of the ESP32-S2 Mini and MAX30102 sensor. The device successfully collects, processes, and transmits biomedical data in real-time, offering a simple and functional solution for basic health monitoring needs.

This project highlights how readily available components can be utilized to design systems that are both effective and easy to use. By combining reliable hardware with straightforward software implementation, I was able to create a device that meets its intended purpose without unnecessary complexity. The wireless communication and web-based interface further enhance the device's usability, making it accessible in a variety of scenarios.

Overall, this project reflects the potential of embedded systems in addressing practical challenges, while also serving as a valuable learning experience in hardware integration, software development, and system design.

Acknowledgment

This article was created in the framework of the National project „IT Academy – Education for the 21st Century“, which is supported by the European Social Fund and the European Regional Development Fund in the framework of the Operational Programme Human Resources, ITMS code of the project: 312011F057.

References

[1] “ESP32 S2 Series Datasheet,” [Online] Available: https://www.espressif.com/sites/default/files/documentation/esp32-s2_datasheet_en.pdf. [Accessed 23 11 2024]

[2] “MAX30205 datasheet,” [Online] Available: https://www.analog.com/media/en/technical-documentation/data-sheets/MAX30205.pdf. [Accessed 27 11 2024].

[3] “LOLIN S2 Mini Development Board Pinout and Technical Specifications,” [Online] Available: https://www.espboards.dev/esp32/lolin-s2-mini/. [Accessed 27 11 2024].

[4] “Arduino Based Digital Thermometer using MAX30205 Human Body Temperature Sensor, “ [Online] Available: https://circuitdigest.com/microcontroller-projects/arduino-max30205-human-body-temperature-measurement. [Accessed 28 11 2024].

[5] “Smart Heart Rate Monitoring with ESP32,“ [Online] Available: https://www.hqonline.com/blog/smart-heart-rate-monitoring-with-esp32. [Accessed 28 11 2024].

[6] “MAX30100 - Heart Rate Oxygen Pulse Sensor,“ [Online] Available: https://components101.com/sensors/max30100-heart-rate-oxygen-pulse-sensor-pinout-features-datasheet. [Accessed 29 11 2024].

[7] https://components101.com/sites/default/files/inline-images/Oximeter-Working.png [Accessed 30 11 2024]

FriStack – Modular System for Educational and Research Purposes

Andrej Šimkovič, Michal Kubaščík, Peter Šarafín, Peter Ševčík

Abstract— This article introduces FriStack, a modular, stackable hardware system designed for IoT applications in educational and research environments. Inspired by existing systems like Seeed Studio's Grove, Adafruit's FeatherWings, and Espressif's M5Stack, FriStack aims to simplify module integration by using a standardized header block for communication. FriStack offers an accessible and less complex alternative to existing systems, while maintaining flexibility for future expansion through modular components. The system's future modules will include wireless communication and AI functionalities to broaden its potential applications in real-time data transmission and processing.

Keywords— stackable system, modularity, ESP32, M5Stack, IoT

I. Introduction

Considering rapid development in the field of IoT applications and implementation in said solutions, we recognize the need to develop a modular, stackable system that can be used in a wide range of applications.

Modularity is a key factor that proves that there is no need to develop one specific hardware solution for one specific need. Instead, it is possible to develop your own solution to your problem using an already-developed system of stackable modules. With this approach it is simpler to create solutions and save time and cost.

While they are mainly used for hobby projects, there is an ambition to expand these systems further into fields of IoT such as smart factory or smart agriculture, where emphasis is laid on data gathering, processing and durability of the system in harsher conditions. Another use could be in education where students could learn embedded programming, IoT and learn to develop their own modules. Furthermore, its capabilities in data collecting and processing and rise of AI implementations could be beneficial in research environment.

II. Stackable Systems

This type of system consists of multiple compatible modules which can be connected without the need for additional soldering. They are used in IoT fields like smart factory or smart home. Additionally, they are used in education as a way to teach about IoT solutions and embedded programming.

The main element of a stackable system is the core which handles communication between modules and users. These modules vary widely in their applications. They can gather data from sensors and use wireless communication methods like Wi-Fi, Bluetooth, and Zigbee. More advanced modules can support AI functionalities such as voice assistants, image recognition, and general data processing. The core and modules are connected with a solderless solution like a header or cable so users can work with it immediately after obtaining it.

Andrej Šimkovič, University of Zilina, Zilina, Slovakia (e-mail: simkovic4@stud.uniza.sk).
Michal Kubaščík, University of Zilina, Zilina, Slovakia (e-mail: michal.kubascik@fri.uniza.sk)
Peter Šarafín, University of Zilina, Zilina, Slovakia (e-mail: peter.sarafin@fri.uniza.sk)
Peter Ševčík, University of Zilina, Zilina, Slovakia (e-mail: peter.sevcik@fri.uniza.sk)

A few of the systems present on the market are:

- Seeed Studio - Grove Ecosystem
- Adafruit - FeatherWings
- Espressif - M5Stack

A. Seeed Studio – Grove Ecosystem

Grove is a modular system categorized as a standardized connector prototyping system. Connections are made through header blocks. It consists of the Base unit which includes a microprocessor which provides communication between the Base unit and the modules using mainly the I2C bus, but some modules are using UART. By communicating through I2C, it is possible to use Grove modules with other systems such as Raspberry Pi or Arduino boards.

The Grove ecosystem offers a broad range of affordable products, making it highly accessible. Seeed Studio offers opportunities to design your own module and sell it on their website. It serves as a significant source of inspiration for our system design as to how this kind of system can work and grow thanks to its community [1].

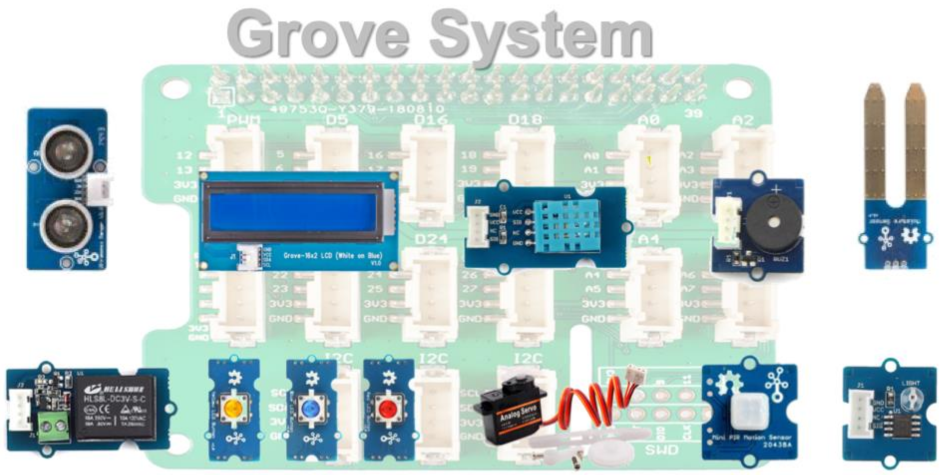

Fig. 1 Grove Ecosystem sensors and extender board [1]

B. Adafruit – FeatherWings

This system comprises the main boards (Feathers) and modules as shields or HATs called Wings. The Feathers have chipsets from various manufacturers such as Atmel, STM, Espressif, SemTech and more are to come.

Wings range from simple sensors to advanced modules like thermal cameras. Almost all Wings are compatible with all Feathers, but because of the usage of so many chipsets in their Feathers the means of available communication changes [2]. For example, GPS Wing is not compatible with Feathers with ESP8266 and nRF52 because this Wing uses UART for communication and these chipsets can't spare their UART as they have only one and are used for programming and debugging [3]. On the other hand, most of the wings use I2C and SPI.

As for programming, it consists of Arduino C/C++ example codes and libraries available for most of the Feathers and FeatherWings. Adafruit provides Feather boards that support CircuitPython, offering an alternative for beginners or those less familiar with Arduino's C/C++ programming language [2].

Unlike Grove Ecosystem this system does not have a standardized cable connector system. So, there is a problem with using different cables for different Wings, but they can be still connected through headers and this method is the default. Another difference is the price of all parts of this system. While Adafruit offers a broader range of chipsets and more complex boards, this level of complexity is beyond what we aim to achieve with our system.

C. *Espressif – M5Stack*

M5Stack began as an idea and personal project of Jimmy Lai and was later bought by the manufacturer of the chipset, which was used in the first M5Stack Core, Espressif. After the purchase, there has been steady growth of IoT solutions and a range of models [4].

The main controller core of the stackable system was M5Stack Core, but they expanded their selection of controllers with controllers of smaller sizes, Stick, Atom and Stamp, but still provide many possibilities of application in IoT [5].

Each of these controllers supports the use of their sensors and modules. Sensors are connected by cables mainly through the I2C bus, but when it comes to modules, they are connected through a universal header which contains all the possibilities of communication of ESP32-S3. However, this mainly applies to M5Stack Core as it is considered their flagship for IoT applications. There is a rich variety of these modules that vary from power supply through communication to camera modules. These modules are not truly stackable as you stack only your Core and then the module. You can use an extender, but you can connect only using connectors and cables.

Additionally, M5Stack solutions can be programmed using various languages like Arduino, MicroPython and UIFlow, which is a drag-and-drop visual programming tool, great for educational purposes and for beginners in embedded programming [5], [6].

This system has complex cores and modules like the FeatherWings boards, but they are more affordable and have unified casing. The casing of each core, sensor and module makes it suitable for harsher environments without the need to develop your own cases for your system [5].

Fig. 2 M5Stack CoreS3 [6]

III. Fristack

For our system, we plan to develop the core which will be less complex than the cores of previously mentioned systems while keeping all possible means of communication between modules. The main idea is that the core would have many uses which would broaden when modules are connected. Another feature would be stackability like FeatherWings by Adafruit. Theoretically, as many modules could be connected to the core until we would run out of power or pins.

The main communication will be through a standardized header block while there will be some I/O connectors for CAN(TWAI) and UART. Also, we plan to include the SPI bus header for possible connection of display or other components.

The power supply of the FriStack will be through USB-C and will be also used for programming and debugging to save space, and cost and fully utilize the properties of ESP32-S3.

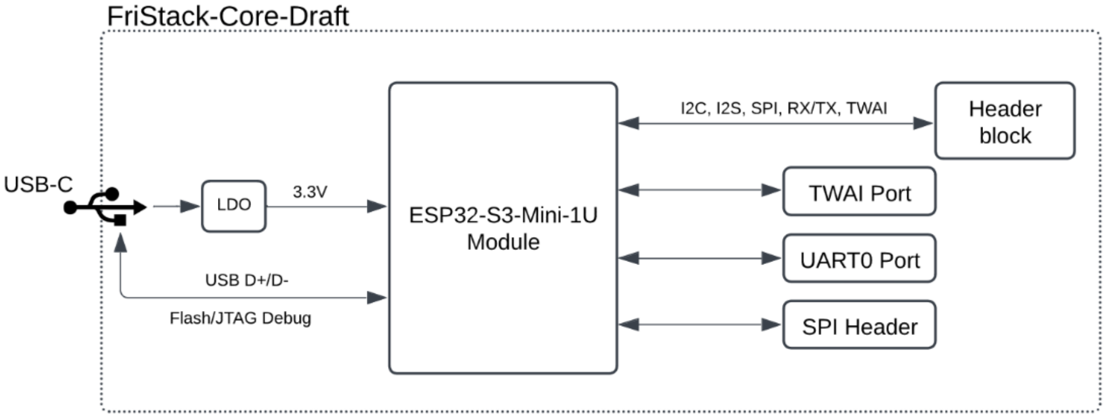

Fig. 3 FriStack block scheme

A. Future modules

To start the project FriStack we would like to offer, with the core of the system, some modules to showcase the possibilities of FriStack and its uses in future applications.

One of them would be a communication module using microcontroller ESP32-C6 thanks to its wireless communication properties. This module could be used for applications where data needs to be transmitted in real-time and cable connection is not practical. Another use could be to connect sensors through Bluetooth and gather data [7].

Another module we are thinking of could be an AI module using ESP32-P4, which is not yet a commercially released model, but it is designed for applications which include image and speech recognition. Due to its high computing power and offer of peripherals, it is a great opportunity to experiment with this microcontroller and its potential [8].

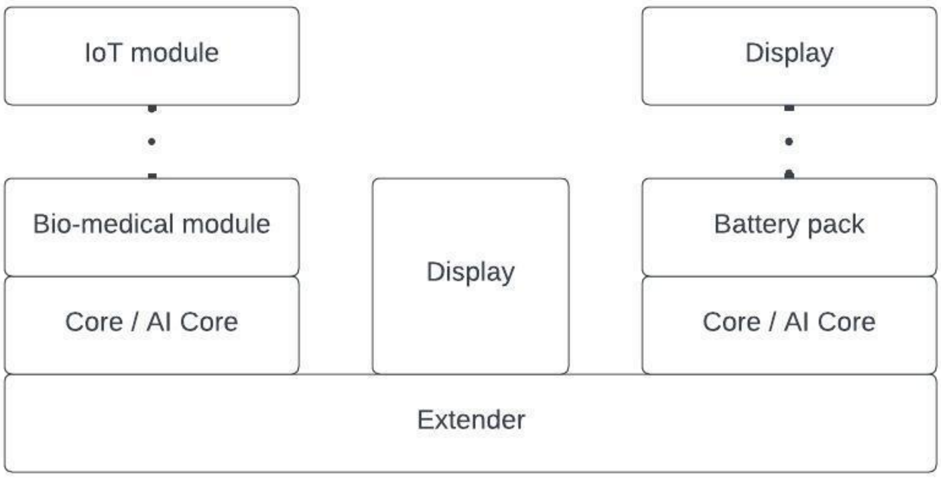

Fig. 4 Example build of FriStack system

B. Standardized header block

As for our project, we mainly get inspiration from Espressif-M5Stack, and we would like to make it compatible with FriStack. We would like to achieve it through an extended module to transform our header to theirs and vice versa.

The header block would consist of peripherals like UART, I2C, I2S and SPI also power and ground would be connected through the header. We also plan to include GPIO pins, pins for flashing core and connected modules as in M5Stack Core3. However, the M5Stack CoreS3 header consists of two 15x2 blocks, we would like to make our header block smaller and possibly just one to conserve the size of our Core and future modules [6].

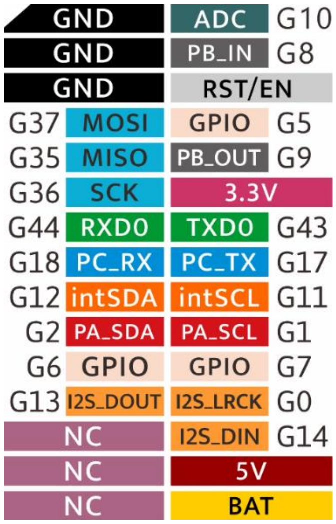

Fig. 5 M5Stack CoreS3 Header blocks

Fig. 6 Concept 3D-model of FriStack

IV. Conclusion

The ambition of our project is to provide a stackable system solution for education and research purposes. We draw inspiration from existing solutions and take a simpler approach to designing to make it more compact, affordable and effective. For now, we want to develop the core of the system that would communicate with all future modules through standardized header block. Additionally, develop a few modules and prepare documentation and methods for future modules development by community as it is going to be open-hardware solution.

References

[1] Seeed Studio, "Grove System," [Online]. Available: https://wiki.seeedstudio.com/Grove_System. [Accessed: Dec. 6, 2024].
[2] Adafruit, "Adafruit Feather Overview," [Online]. Available: https://learn.adafruit.com/adafruit-feather/overview. [Accessed: Dec. 6, 2024].
[3] Adafruit, "Adafruit Feather GPS Wing," [Online]. Available: https://learn.adafruit.com/adafruit-feather/gps-wing. [Accessed: Dec. 6, 2024].
[4] M5Stack, "About Us," [Online]. Available: https://m5stack.com/about-us. [Accessed: Dec. 6, 2024].
[5] M5Stack, "Product Documentation," [Online]. Available: https://docs.m5stack.com/en/products. [Accessed: Dec. 6, 2024].
[6] M5Stack, "CoreS3," [Online]. Available: https://docs.m5stack.com/en/core/CoreS3. [Accessed: Dec. 6, 2024].
[7] Espressif, "ESP32-C6 Datasheet," [Online]. Available: https://www.espressif.com/sites/default/files/documentation/esp32-c6_datasheet_en.pdf. [Accessed: Dec. 6, 2024].
[8] Espressif, "ESP32-P4," [Online]. Available: https://www.espressif.com/en/products/socs/esp32-p4. [Accessed: Dec. 6, 2024].

Energy Storage Systems - a Way of Increasing Operational Time of WSN Devices

Tomáš Bača, Ján Šumský, Michal Kubaščík, Peter Šarafín

***Abstract*—**The increasing demand for sustainable and efficient energy solutions have led to significant advancements in energy storage systems. This paper provides a comprehensive overview of various energy storage technologies, including thermal energy storage (TES), mechanical energy storage (MES), chemical energy storage (CES), battery energy storage (BES), and electrical energy storage (EES). We explore specific methods such as molten salt, aquifer, and thermochemical systems for TES; pumped hydro, gravity, compressed air, and flywheel systems for MES; hydrogen, synthetic natural gas, and solar fuels for CES; and a range of battery types, including lithium-ion, lead-acid, nickel-cadmium, sodium sulfur, sodium ion, and metal-air. Additionally, we examine emerging technologies like paper batteries, advanced capacitors, and supercapacitors for EES. The paper concludes with a comparative analysis of this storage systems and discusses the most promising directions for the future energy storage solutions.

***Keywords*—**Energy storage systems, Thermal energy storage, Mechanical energy storage, Chemical energy storage, Electrochemical energy storage, Electrical energy storage

I. INTRODUCTION

The rapid increase in global energy consumption, driven by industrialization, technological advancements, and economic growth, particularly in developing countries, has intensified the need for efficient and sustainable energy solutions. According to the International Energy Agency (IEA), global energy demand surged by 4.5\% in 2021, significantly contributing to the rise in CO2 emissions. To combat this environmental challenge, renewable energy sources are being deployed at an unprecedented rate, aiming to reduce greenhouse gas emissions. Renewable energy, notably from photovoltaic cells, wind turbines, and hydropower plants, reached record levels in 2021, accounting for a significant portion of the global energy generation. [1]

However, the inherent intermittency of renewable energy sources, such as the variability of solar and wind power, poses challenges in maintaining a consistent energy supply. Energy storage systems (ESSs) have emerged as a crucial technology to address these challenges by storing excess energy and ensuring a reliable energy supply when renewable sources are insufficient.

ESSs encompass a diverse range of technologies, each with unique applications and benefits. These systems include thermal, mechanical, chemical, battery, and electrical storage methods, all designed to optimize energy management and mitigate energy spillage. Despite the extensive research on ESSs, reviews often focus on specific types, leaving a gap in comprehensive studies covering all major storage technologies.

This paper aims to provide an in-depth review of the various energy storage systems, highlighting their evolution, classifications, current status, characteristics, and applications. By assembling comprehensive information on ESSs, this review seeks to offer valuable insights for researchers and industry professionals, guiding future developments in the field of energy storage. [2]

Tomáš Bača, University of Žilina, Slovak Republic (e-mail: tomas.baca@fri.uniza.sk)
Ján Šumský, University of Žilina, Slovak Republic (e-mail: jan.sumsky@fri.uniza.sk)
Michal Kubaščík, University of Žilina, Slovak Republic (e-mail: michal.kubascik@fri.uniza.sk)
Peter Šarafín, University of Žilina, Slovak Republic (e-mail: peter.sarafin@fri.uniza.sk)

II. THERMAL ENERGY STORAGE (TES) SYSTEM

Thermal energy storage (TES) systems are engineered to store heat energy by processes such as cooling, heating, melting, condensing, or vaporizing a substance. Depending on the temperature range, these materials are stored at either high or low temperatures in insulated containers. The stored energy can later be recovered for various applications, including residential and industrial uses like space heating or cooling, hot water production, or electricity generation.

TES systems are employed for diverse purposes, ranging from industrial cooling below -18°C, building cooling between 0 and 12°C, heating buildings between 25 and 50°C, to industrial heat storage over 175°C. TES technologies are broadly categorized into low-temperature energy storage (LTES) and high-temperature energy storage (HTES), based on the operating temperature of the storage material relative to the ambient temperature. [3]

LTES systems include aquifer thermal energy storage (ATES) and cryogenic energy storage. In ATES, water is cooled or frozen during periods of low energy demand and later used to meet cooling requirements during peak demand periods. Cryogenic energy storage involves the use of cryogens, such as liquid nitrogen or liquid air, which are boiled using ambient heat and subsequently used to generate electricity through a cryogenic heat engine. LTES is well-suited for high-power density applications, such as load shaving, industrial cooling, and future grid power management.

HTES systems often involve the use of materials like molten salts, which can store and release substantial amounts of thermal energy at high temperatures, making them ideal for electricity generation and industrial processes.

This section will explore different types of TES systems, focussing on molten salt thermal energy storage (HTES), aquifer thermal energy storage (ATES), and thermochemical energy storage (TCES) systems, highlighting their principles, advantages, and applications.

A. Molten salt thermal energy storage system

Molten salts are highly effective for storing sensible heat at temperatures exceeding 100 °C. These salts are liquids formed by melting inorganic salts, and they offer several advantages, including high boiling points, low viscosity, low vapour pressure, and high volumetric heat capacities. The low vapour pressure allows for storage solutions that do not require pressurized vessels, and the high volumetric heat capacity reduces the required storage tank space.

Molten salts are widely used in concentrated solar power (CSP) plants, which utilize parabolic troughs or heliostats to concentrate sunlight. Due to the high demand for molten salts in the CSP industry, extensive research has been conducted to identify suitable molten salt mixtures for both heat transfer fluids (HTFs) and thermal energy storage (TES) materials. The market for molten salt thermal energy storage is expected to expand significantly during the coming years.

Common molten salt fluids include solar salts, Hitec, and Hitec XL. These mixtures are frequently used due to their optimal properties for thermal storage. Molten salt energy storage systems are typically configured in two ways: two-tank direct and two-tank indirect systems. In a direct storage system, molten salt functions as both the heat transfer fluid, absorbing heat from the reactor or heat exchanger, and the storage medium. In contrast, an indirect system uses a separate medium to store heat, with molten salt acting only as the HTF.

These systems employ two tanks: one for cold storage and one for hot storage. The cold tank typically operates at temperatures between 280°C and 290°C, while the hot tank operates between 380°C and 550°C.

In this system, the heater converts renewable energy into heat. In the hot tank is stored the heated molten salt that is heated by the circulation of cooled molten salt from the cold tank through the heater. When we want to release the energy stored in the hot tank, we circulate the heated molten salt from the hot tank through the steam generator. The steam from this generator can be directly used to heat buildings or power steam turbines inside electricity generators. The cooled molten salt from the stem generator is returned to the cold tank for later use.

The size and number of tanks depend on the storage capacity, with commercial operations commonly using tanks with heights of 12–14 meters and diameters exceeding 35 meters.

B. Aquifer thermal energy storage (ATES) system

Aquifer thermal energy storage (ATES) involves the use of permeable rock layers, or aquifers, to store and convey groundwater for heating and cooling purposes. ATES is a form of sensible seasonal storage, where groundwater is extracted and injected through at least two hydraulically connected wells and a heat pump. One well stores warm water (approximately 14–16°C) and the other stores cold water (approximately 5–10°C). These wells can be arranged horizontally (doublet) or vertically within a single borehole (monowell). The critical distance between the wells is determined by factors such as well production rates, aquifer thickness, and the hydraulic and thermal properties governing the storage volume.

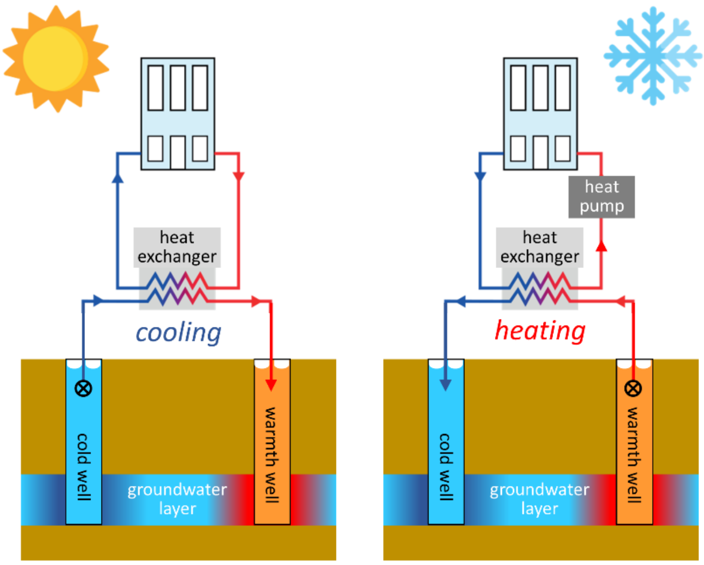

Figure 1 - Schematic ATES system

In a large-scale ATES system, multiple wells are used in a multi-well configuration. During the summer, groundwater from the cold well is used for cooling, and the resulting warm water is fed back into the warm well. In winter, the process is reversed: groundwater from the warm well is heated further to around 40–50°C for heating purposes, and the cooled water is returned to the cold well. Both wells are often equipped with heat pumps to facilitate the bidirectional flow of water. The efficiency of energy storage with ATES is highly dependent on the geological characteristics of the site.

C. Thermochemical energy storage (TCES) system

Thermochemical energy storage (TCES) systems store heat energy indirectly through reversible chemical reactions, unlike sensible heat storage (SHS) or latent heat storage (LHS). In TCES, heat is absorbed and released during the dissociation and association of molecular bonds in an endothermic and exothermic reaction, respectively. The stored heat energy is determined by the type and quantity of the storage material, the enthalpy of the reaction, and the degree of conversion of the reactants.

During an endothermic reaction, heat is stored as reactive components dissociate into individual components. This stored energy is later released in an exothermic reaction when the components recombine. Key parameters for selecting thermochemical materials include energy density and reaction temperature, which are crucial for practical applications. Promising thermochemical storage materials and their respective properties, such as energy density and reaction temperature, are listed in relevant research tables.

Various review articles have assessed the potential applications of TCES and identified challenges impeding its maturity. For instance, research has evaluated the technical properties of cobalt, manganese, and copper oxide-based TCES systems in terms of energy density and cycle life. These studies aim to advance the development and deployment of TCES technologies.

III. MECHANICAL ENERGY STORAGE (MES) SYSTEM

Mechanical energy storage (MES) systems store energy by converting electrical energy into mechanical energy, which can be stored in the form of potential or kinetic energy. When energy demand is low during off-peak hours, the electrical energy from the grid is transformed and stored as mechanical energy. During peak hours, this mechanical energy is converted back into electrical energy to meet the increased demand. MES systems are categorized into four main types: pumped hydroelectric energy storage (PHES), gravity energy storage (GES), compressed air energy storage (CAES), and flywheel energy storage (FES). PHES, GES, and CAES store energy as potential energy, while FES stores it as kinetic energy. One of the main advantages of MES systems is their ability to quickly convert and release stored mechanical energy. [5]

A. Pumped hydroelectric energy storage (PHES) system

The pumped hydroelectric energy storage (PHES) system is the most widely used mechanical energy storage system due to its large energy capacity, long storage duration, and high efficiency. A typical PHES system consists of two large water reservoirs situated at different elevations, a pump to move water from the lower reservoir to the upper reservoir, and a turbine to generate electricity as water flows back down. During off-peak hours, electrical energy is used to pump water to the higher reservoir, storing energy as gravitational potential energy. During peak demand, the stored water is released back to the lower reservoir, passing through turbines to generate electricity. The energy storage capacity of a PHES system is determined by the volume of water reservoirs and the height difference between the reservoirs.

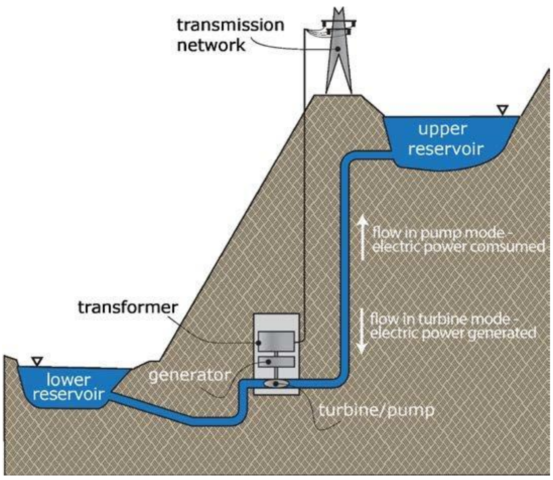

Figure 2 - Schematic of pumped storage hydropower system [6]

Innovations in PHES technology include underground PHES (UPHES) and seawater PHES (SPHES). UPHES uses abandoned quarries or mines as lower reservoirs, while SPHES uses the sea as lower reservoirs, reducing construction costs and environmental impact. Additionally, variable-speed PHES, employing asynchronous motor generators, allows for better control of the pump/turbine speed, enhancing energy absorption during the pumping cycle. These advancements aim to improve the efficiency and feasibility of PHES systems.

B. Gravity energy storage (GES) system

Gravity energy storage (GES) systems have emerged as an alternative to PHES, particularly in regions with geological limitations and water scarcity. GES systems store energy by using gravitational potential energy. The basic concept involves lifting a heavy object, such as a piston, using excess electrical energy during off-peak hours. When energy is needed, the object is allowed to fall, driving a generator to produce electricity.

A typical GES system comprises a large piston in a water-filled shaft, connected to a powerhouse with a pump, turbine, and motor/generator. During charging, the pump lifts the piston by moving water into the shaft. During discharging, the falling piston forces water through the turbine, generating electricity. The storage capacity of GES systems depends on the mass of the piston and the height of the shaft. This technology aims to provide power in the range of 40 MW to 1.6 GW, offering a flexible and scalable energy storage solution.

C. Compressed air energy storage (CAES) system

Compressed air energy storage (CAES) systems store energy by compressing air and storing it in underground caverns or reservoirs. The amount of energy stored depends on the volume, pressure, and temperature of the compressed air. CAES systems offer a reliable and economically feasible alternative to PHES, with lower environmental impacts.

A typical CAES system includes a motor-driven compressor, a multi-stage compressor, a storage cavern, high- and low-pressure turbines, and a generator. During off-peak hours, surplus electricity drives the compressor, which compresses air and stores it in the cavern. During peak demand, the compressed air is released, driving the turbines to generate electricity. CAES systems can store large amounts of energy and provide grid stability, making them an important component of modern energy storage infrastructure.

D. Flywheel energy storage (FES) system

Flywheel energy storage (FES) systems store energy in the form of kinetic energy, utilizing the rotational energy of a massive rotating cylinder. A modern FES system consists of a flywheel, magnetic bearings, an electrical motor/generator, a power conditioning unit, and a vacuum chamber. The motor/generator is reversible, acting as a motor to spin the flywheel during charging and as a generator to convert kinetic energy back into electrical energy during discharging.

FES systems are classified into low-speed and high-speed categories. Low-speed FES systems use steel flywheels rotating at speeds below 6,000 rpm, while high-speed FES systems use advanced composite materials for flywheels that rotate at speeds up to 100,000 rpm. FES systems offer rapid response times, high power density, and long cycle life, making them suitable for applications requiring frequent and rapid energy storage and retrieval.

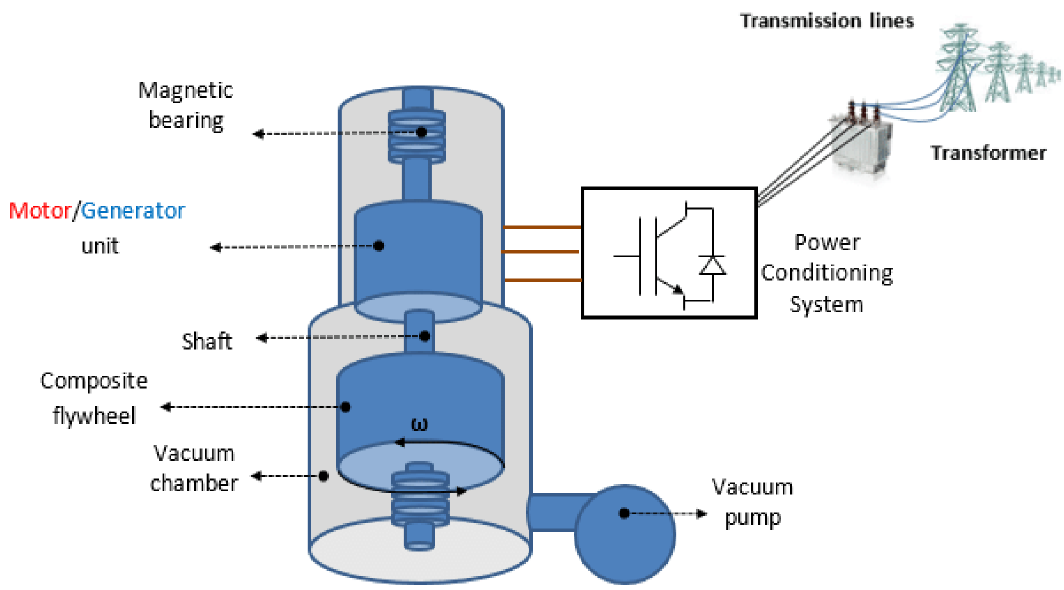

Figure 3 - Schematic of flywheel energy storage system [7]

IV. CHEMICAL ENERGY STORAGE (CES) SYSTEM

Chemical energy storage (CES) systems are particularly effective for long-term energy storage. These systems store energy in the chemical bonds between atoms and molecules, releasing this stored energy through chemical reactions. During this process, the materials' composition changes as original chemical bonds break and new ones form. Chemical fuels play a significant role in both electricity generation and the transportation industry worldwide. Common chemical fuels include coal, petrol, diesel fuel, natural gas, liquefied petroleum gas (LPG), propane, butane, ethanol, and hydrogen. These fuels are first converted into mechanical energy and subsequently into electrical energy, which is then used for power generation. CES systems mainly encompass hydrogen, synthetic natural gas (SNG), and solar fuel storage systems.

A. Hydrogen energy storage system

Hydrogen is considered an ideal energy carrier due to its clean and carbon-free nature, making it a zero-emission chemical energy carrier. Hydrogen can be produced from water via electrolysis or directly from sunlight through photocatalytic water splitting. A typical hydrogen energy system includes three main components: a hydrogen generation unit (such as an electrolyser) to convert electrical energy into hydrogen, a hydrogen storage system, and a hydrogen energy conversion unit (such as a fuel cell) to convert the stored chemical energy in hydrogen back into electrical energy. This versatile approach to energy storage offers significant potential for clean and sustainable energy solutions.

B. Synthetic natural gas (SNG)

Natural gas is a widely used and relatively clean energy source among fossil fuels. The conversion of coal to synthetic natural gas (SNG) has been established as a viable alternative for energy production. Biomass can also be used to produce SNG, presenting a carbon-neutral option. The methanation process, initially used in the 1960s and 1970s, converts coal into SNG. Recent advancements have developed new thermal gasification processes to produce SNG from coal and dry biomass, involving multiple conversion steps such as drying, gasification, gas cleaning, and methanation of producer gas. SNG can be stored in pressurized tanks, underground caverns, or fed directly into the gas grid. An example of this technology in practice is the Great Plains Synfuels Plant (GPSP) in North Dakota, USA, which has been producing approximately 4.1 million m^3/day of SNG from lignite coal since 1984.

C. Solar fuels

Solar fuels aim to capture the sun's abundant energy, convert it into usable forms, store it in chemical bonds, and utilize it as needed. There are three main approaches to producing solar fuels: natural photosynthesis, artificial photosynthesis, and thermochemical production.

Natural photosynthesis is the process by which plants, algae, and some bacteria convert solar energy into fuel, storing it in carbohydrates. These carbohydrates act as fuels that support plant growth and maintenance. Artificial photosynthesis mimics this natural process, capturing sunlight and using it to chemically convert water and carbon dioxide into fuels, resulting in solar fuels. The term ”artificial leaf” refers to this process, which aims to produce fuels using solar energy. Thermochemical production involves using sunlight to heat materials to very high temperatures, where they react with steam or CO2 to produce hydrogen or carbon monoxide, which can then be used as fuels.

V. BATTERY ENERGY STORAGE (BES) SYSTEM

Batteries are electrochemical devices that convert chemical energy into electrical energy. They consist of multiple cells, each with three primary components: an anode, a cathode, and an electrolyte. Batteries are broadly categorized into two types: primary and secondary. Primary batteries are single-use and cannot be recharged once their chemical energy is depleted. Secondary batteries, however, are rechargeable. Depending on the materials used for the electrodes and electrolyte, secondary batteries are classified into various types, including lead-acid (LA), lithium-ion (Li-ion), nickel-cadmium (Ni-Cd), sodium-sulphur (NaS), sodium-ion (Na-ion), and metal-air batteries. Each type has its own specific characteristics and applications. [8]

A. Lithium-ion (Li-ion) batteries

Li-ion batteries are widely used in electronics and the transportation industry, particularly in power grid applications and plug-in hybrid electric vehicles, due to their high charge density. These rechargeable batteries have a lithium metal oxide cathode, a graphitic carbon anode, and an electrolyte containing dissolved lithium salts. During charging, lithium ions move from the cathode to the anode, where they are stored. During discharge, the process reverses, releasing energy.

B. Lead-acid (LA) batteries

Lead-acid batteries are among the oldest and most established types of rechargeable batteries. They consist of lead dioxide as the cathode, sponge lead as the anode and sulphuric acid as the electrolyte. They are commonly used in automotive starters and backup power systems due to their reliability and low cost.

C. Nickel-cadmium (Ni-Cd) batteries

Nickel-cadmium batteries have a nickel oxide hydroxide cathode, a cadmium anode, and an alkaline electrolyte. They are known for their robustness and long life cycle. These batteries are used in various applications, including emergency lighting and portable power tools.

D. Sodium sulphur (NaS) batteries

Sodium-sulphur batteries consist of a liquid sodium anode and a liquid sulphur cathode, separated by a solid ceramic electrolyte. These batteries operate at high temperatures and are used for grid energy storage due to their high energy density and efficiency.

E. Sodium-ion (Na-ion) batteries

Sodium-ion batteries use sodium ions as charge carriers, with a sodium metal oxide cathode, a hard carbon anode, and an electrolyte containing sodium salts. They are considered a potential alternative to Li-ion batteries due to the abundance and low cost of sodium.

F. Metal-air batteries

Metal-air batteries generate electricity through the oxidation of a metal (such as zinc or aluminium) with oxygen from the air. They have a high energy density and are used in applications requiring long-term energy storage and high energy output.

VI. PAPER BATTERIES

Paper batteries are innovative energy storage devices made primarily of paper or cellulose and carbon nanotubes. They are ultra-thin, flexible, non-corrosive, and require minimal housing. Their flexibility allows them to be bent, twisted, or wrapped around objects, making them ideal for fitting into tight spaces and reducing overall system size and weight.

A typical paper battery consists of a sheet of paper coated with an ionic solution and smeared with carbon nanotube ink as the cathode. On the other side, a thin layer of lithium serves as the anode, and aluminium rods on each side carry the current.

Various types of paper batteries have been developed for different applications. For example, coating cellulose paper with materials of opposite electrochemical potentials generates voltage, with a simple Cu/paper/Al combination producing 0.5 V. Recent advancements include water-activated paper batteries using activated carbon as the anode, where power output is proportional to the carbon load.

Recent research highlights breakthroughs in paper-based electrodes and their use in flexible energy storage devices. Studies also explore the potential of paper batteries in point-of-care testing, environmental monitoring, and food safety.

Overall, paper batteries offer a flexible, lightweight, and environmentally friendly alternative to traditional batteries.

VII. ELECTRICAL ENERGY STORAGE (EES) SYSTEM

Electrical energy storage (EES) systems store energy in an electric field without converting it into other forms of energy. They are broadly classified into two types: electrostatic energy storage systems and magnetic energy storage systems. Capacitors and supercapacitors fall under electrostatic energy storage systems, while superconducting magnetic energy storage (SMES) represents magnetic energy storage systems.

A. Capacitors

Capacitors are fundamental components in EES systems, known for their ability to store electrical energy using an electrostatic field. A typical capacitor comprises two conductive metal plates separated by a dielectric material (an insulating layer), as illustrated in Fig. 48. When a voltage is applied across the plates, an electric field develops in the dielectric, causing one plate to accumulate positive charge and the other plate to accumulate negative charge. This arrangement allows the capacitor to store energy in the electrostatic field between the plates.

Capacitors are characterized by their rapid charge and discharge capabilities, making them ideal for applications requiring short bursts of energy. However, they have a relatively low energy density compared to other storage technologies, limiting their use to applications such as power conditioning, signal processing, and coupling/decoupling in electronic circuits.

B. Supercapacitors

Supercapacitors, also known as electric double-layer capacitors (EDLCs) or ultracapacitors, represent a significant advancement in capacitor technology. They consist of two electrodes, typically made of activated carbon, an electrolyte, and a separator. The electrodes are porous, providing a large surface area for charge storage, which significantly enhances the energy density compared to conventional capacitors.

In supercapacitors, energy is stored in the form of an electrostatic field created by the separation of charges at the interface between the electrode material and the electrolyte. When a voltage is applied, ions in the electrolyte move towards the electrode of opposite charge, forming a double layer of charge. This mechanism allows supercapacitors to achieve much higher capacitance values.

Supercapacitors are particularly useful in applications requiring rapid energy delivery and high power density. They are used in hybrid electric vehicles (HEVs), renewable energy systems, and various high-power applications such as backup power supplies and power stabilization.

The development of supercapacitors has been driven by advances in materials science, particularly in the use of carbon-based materials with high specific surface areas and novel electrolytes. These materials allow for the fabrication of supercapacitors with enhanced performance characteristics, such as higher energy density, better cycle life, and improved thermal stability.

Supercapacitors bridge the gap between traditional capacitors and batteries. They offer higher energy densities than conventional capacitors and can deliver more power than batteries, albeit with lower overall energy storage capacity. This makes them ideal for applications where both high power and rapid charge/discharge cycles are required.

C. Superconducting Magnetic Energy Storage (SMES) System

Superconducting magnetic energy storage (SMES) systems store energy in the magnetic field generated by a direct current (DC) flowing through a superconducting coil. The superconductivity principle, discovered in 1911, enables these systems to operate with zero electrical resistance, allowing highly efficient energy storage. The first SMES concept was proposed by Ferrier in 1969 for large-scale energy storage, and practical research began in 1971 at the University of Wisconsin. The first commercial SMES application in a power grid was implemented in 1981 along the 500 kV Pacific Intertie in the United States.

An SMES system comprises three primary components: a superconducting coil, a control and power conditioning system, and a cryogenically cooled refrigeration system.

Superconducting Coil: The coil is made from superconducting materials, such as niobium-titanium (Nb-Ti) or high-temperature superconductors (HTS). To maintain superconductivity, the coil must be cooled to cryogenic temperatures using liquid helium or other cooling techniques. The superconducting state allows the coil to conduct electricity without resistance, minimizing energy loss.

Control and Power Conditioning System: This system manages the charging and discharging cycles of the SMES. It regulates the flow of current to and from the superconducting coil, ensuring that the system operates efficiently. It also includes power conversion equipment to switch between alternating current (AC) and direct current (DC) as needed.

Cryogenic Cooling System: The superconducting coil is maintained at cryogenic temperatures to ensure it remains in a superconducting state. This is achieved using a refrigeration system that continuously cools the coil, typically with liquid helium for low-temperature superconductors or liquid nitrogen for HTS.

During the charging phase, a DC current is passed through the superconducting coil, generating a magnetic field and storing energy. When energy is needed, the current is decreased, and the magnetic field collapses, releasing the stored energy back into the electrical grid. The energy stored in an SMES system is proportional to the square of the current and the inductance of the coil.

SMES systems are characterized by their rapid response times (in milliseconds), high power output (multi-megawatts), and high efficiency (near 100\%). These attributes make SMES particularly suitable for applications in power systems that require fast and reliable energy delivery, such as grid stabilization, frequency regulation, and load leveling.

VIII. COMPARISON AMONG THE ENERGY STORAGE SYSTEMS

In this section, we present a comparative review of various energy storage systems (ESS) that have been discussed in the preceding sections. Energy storage systems play a crucial role in modern energy management, providing solutions for balancing supply and demand, enhancing grid stability, and supporting the integration of renewable energy sources. Each storage technology has distinct characteristics, making it suitable for specific applications.

The comparison is based on several key parameters, including energy density, response time, cost, and typical applications. Energy density refers to the amount of energy stored per unit volume or mass, which affects the capacity and size of the storage system. Response time measures how quickly the storage system can release or absorb energy, which is critical for applications requiring immediate power. The cost encompasses both the initial investment and operational expenses, influencing the economic feasibility of the storage technology. Typical applications highlight the common uses and scenarios where each technology excels.

The following table provides a summarized comparison of the various energy storage systems, allowing for an easy understanding of their strengths and weaknesses in different contexts.

Table 1 - Comparison of energy storage systems

Storage system	**Energy density**	**Response time**	**Cost**	**Typical applications**
Molten salt TES	High	Slow	Medium	Solar thermal power plants
ATES	Medium	Slow	Low	Seasonal storage, building heating
TCES	High	Slow	Medium	Industrial processes
PHES	High	Medium	High	Grid storage, load leveling
GES	Medium	Medium	Medium	Grid storage (future potential)
CAES	Medium	Medium	Medium	Large-scale energy management
FES	Low	Fast	High	Grid stabilization, short-term storage
Hydrogen	High	Slow	High	Energy storage, fuel for transport

SNG	Medium	Slow	High	Energy production, grid storage
Solar fuels	High	Slow	High	Sustainable energy (future potential)
Li-ion batteries	High	Fast	High	Electronics, electric vehicles
Lead-acid batteries	Low	Medium	Low	Automotive, backup power
Ni-Cd batteries	Medium	Medium	Medium	Industrial applications
NaS batteries		Medium	Medium	Grid storage
Na-ion batteries	Medium	Medium	Medium	(Developing technology)
Metal-air batteries	High	Medium	Medium	(Experimental, future potential)
Paper batteries	Low	Medium	Low	Flexible electronics (developing)
Capacitors	Low	Very Fast	Low	Short-term power demands
Super-capacitors	Medium	Very Fast	Medium	Regenerative braking, power smoothing
SMES	Medium	Very Fast	High	Grid stabilization, power quality

IX. PROMISING WAY TO STORE ENERGY

The evolution of energy storage technologies is critical to meeting the demands of a world increasingly reliant on renewable energy sources. Each energy storage system (ESS) has its unique advantages, and the Technology Readiness Level (TRL) framework helps gauge their development stages and commercialization readiness.

As we evaluate promising energy storage solutions, it's essential to understand their current status and potential. Technologies like lead-acid, lithium-ion, and nickel-cadmium batteries have reached high levels of maturity and are widely deployed in various applications due to their reliability and established performance. Pumped hydro energy storage (PHES) and low-speed flywheel energy storage systems are also well-established, demonstrating their effectiveness in large-scale and grid stabilization applications.

Emerging technologies such as electric double-layer capacitors (EDLC) and advanced compressed air energy storage (CAES) systems are progressing rapidly. These technologies are promising due to their potential for improved performance and scalability. Additionally, hydrogen storage systems, despite their high costs, offer significant future potential due to their versatility and ability to support sustainable energy solutions.

Thermal energy storage methods, including molten salt, aquifer, and thermochemical storage, are gaining attention for their ability to store and dispatch energy effectively over long periods. These methods are particularly suitable for balancing energy supply with demand in renewable energy applications.

As the energy landscape evolves, ongoing research and development will likely drive advancements in these technologies. The focus will continue to be on enhancing efficiency, reducing costs, and expanding the range of applications. By advancing these promising storage solutions, we can better address the challenges of integrating intermittent renewable energy sources and support a more sustainable energy future.

X. CONCLUSION

The transition to renewable energy sources presents significant challenges due to their intermittent nature. Effective energy storage systems (ESS) are crucial for ensuring a stable and reliable energy supply, addressing the gaps between energy production and consumption.

This review has explored a range of ESS technologies, each with its specific characteristics and applications. For large-scale energy management, technologies like pumped hydro storage and thermal energy storage are highly effective. Battery technologies, including lithium-ion and lead-acid batteries, offer robust solutions for various power needs, from electronics to electric vehicles. Supercapacitors, SMES, and flywheel systems excel in applications requiring rapid response and short-duration energy storage.

While hydrogen and synthetic natural gas (SNG) present exciting future possibilities, they currently face challenges related to efficiency and cost. However, their potential for large-scale energy storage remains significant. As research progresses, these technologies may become more viable and cost-effective.

In summary, the advancement and deployment of diverse energy storage technologies are essential for optimizing energy systems and supporting the shift towards renewable energy. Continued innovation and development in these areas will play a pivotal role in meeting future energy needs and achieving sustainability goals.

REFERENCES

[1] J. Mitali, S. Dhinakaran, and A. Mohamad, "Energy storage systems: a review," *Energy Storage and Saving*, vol. 1, no. 3, pp. 166–216, Sep. 2022. [Online]. Available: https://www.sciencedirect.com/science/article/pii/S277268352200022X. Accessed: Dec. 6, 2024.

[2] F. Nadeem, S. M. S. Hussai, and P. K. Tiwari, "Comparative review of energy storage systems, their roles, and impacts on future power systems," *IEEE Access*, vol. 7, pp. 4555–4585, Dec. 2018. [Online]. Available: https://ieeexplore.ieee.org/document/8580457. Accessed: Dec. 6, 2024.

[3] D. Akinyele and R. Rayudu, "Review of energy storage technologies for sustainable power networks," *Sustainable Energy Technologies and Assessments*, vol. 8, pp. 74–91, Dec. 2014. [Online]. Available: https://www.sciencedirect.com/science/article/pii/S2213138814000708. Accessed: Dec. 6, 2024.

[4] Wageningen, "Aquifer thermal energy storage." [Online]. Available: https://www.wur.nl/en/show/aquifer-thermal-energy-storage.htm. Accessed: Dec. 6, 2024.

[5] E. Hossain, H. M. R. Faruque, M. S. H. Sunny, N. Mohammad, and N. Nawar, "A comprehensive review on energy storage systems: Types, comparison, current scenario, applications, barriers, and potential solutions, policies, and future prospects," *Energies*, vol. 13, no. 14, pp. 1–127, Jul. 2020. [Online]. Available: https://www.mdpi.com/1996-1073/13/14/3651. Accessed: Dec. 6, 2024.

[6] R. C. Viadero Michele, R. Rehbein Anshu, and S. Singh, "Hydropower on the Mississippi River," 2017. [Online]. Available: https://www.researchgate.net/publication/318469208_Hydropower_on_the_Mississippi_River. Accessed: Dec. 6, 2024.

[7] P. Nikolaidis and A. Poullikkas, "A comparative review of electrical energy storage systems for better sustainability," *Journal of Power Technologies*, vol. 97, no. 3, pp. 220–245, 2017. [Online]. Available:

https://www.researchgate.net/publication/320755664_Journal_of_Power_Technologies_97_3_2017_220-245_A_comparative_review_of_electrical_energy_storage_systems_for_better_sustainability. Accessed: Dec. 6, 2024.

[8] S. Koohi-Fayegh and M. Rosen, "A review of energy storage types, applications and recent developments," *Journal of Energy Storage*, vol. 27, Feb. 2020. [Online]. Available: https://www.sciencedirect.com/science/article/pii/S2352152X19306012. Accessed: Dec. 6, 2024.

Intelligent Power Socket

Štefan Blahovec, Michal Hodoň, Lukáš Čechovič

***Abstract*—**This paper presents the development of a smart socket designed to monitor and control household energy consumption through the Internet of Things (IoT). The system integrates an ESP32 microcontroller, sensors, and an MQTT-based communication protocol to enable real-time energy monitoring and remote control of connected appliances. An intuitive web-based interface allows users to access and manage energy data efficiently. The system was tested under various conditions to evaluate its accuracy, reliability, and scalability. Results demonstrate the smart socket's potential for enhancing energy efficiency and facilitating sustainable energy practices in residential settings.

***Keywords*—**smart socket, Internet of Things (IoT), energy measurement, remote control, smart home.

I. Introduction

The growing emphasis on energy conservation and sustainable practices has highlighted the need for efficient household energy management systems. Residential electricity consumption accounts for a significant proportion of global energy use, and the ability to monitor and control appliances in real time is essential for reducing energy waste and optimizing consumption patterns [1][2]. Traditional energy monitoring systems, while effective, often lack accessibility and user-friendliness, limiting their adoption in everyday households. Advances in IoT technology provide a solution by enabling connected devices to gather, transmit, and analyze data seamlessly, empowering users to make informed energy-saving decisions [3].

Smart sockets represent an innovative application of IoT in energy management, offering a versatile and cost-effective solution for monitoring and controlling electrical appliances. By integrating real-time energy monitoring, remote control, and automation capabilities, smart sockets help users optimize their energy consumption and contribute to sustainability goals. Recent studies have demonstrated the effectiveness of IoT-enabled devices in reducing energy waste and enhancing user engagement in energy management [4][5]. However, challenges such as scalability, data reliability, and integration with existing systems remain significant barriers to widespread adoption.

This paper introduces a smart socket system designed to address these challenges. The system utilizes an ESP32 microcontroller as its core, incorporating sensors to measure energy consumption and an MQTT-based communication protocol for efficient data transmission. The system is complemented by a web-based interface that enables users to monitor energy usage and control appliances remotely. By combining cost-effective hardware with intuitive software, the proposed smart socket aims to provide an accessible solution for real-time energy management in residential environments.

II. Integration

The integration of sensors and the ESP module significantly enhances the smart socket's functionality by providing comprehensive monitoring and control capabilities. A key component in this integration is the current sensor, specifically the ACS712 -30A Hall effect current sensor, which measures the current and power consumption of devices connected to the smart sockets [2]. This data is crucial for users to monitor and manage their energy usage effectively, preventing wastage and promoting energy efficiency. Additionally, the NodeMCU, which is based on the ESP8266-12E Wi-Fi module, acts as the central control unit, facilitating

Štefan Blahovec, University of Zilina, Zilina, Slovakia (e-mail: blahovec6@stud.uniza.sk)
Michal Hodoň, University of Zilina, Zilina, Slovakia (e-mail: michal.hodon@fri.uniza.sk)
Lukáš Čechovič, University of Zilina, Zilina, Slovakia (e-mail: lukas.cechovic@fri.uniza.sk)

remote control and automation of the smart sockets [2]. This module processes data received from the server and allows users to interact with their smart sockets through a web interface, providing a seamless user experience. Furthermore, the integration of the relay module, activated by the NodeMCU, enables the physical control of the power supply to connected devices, allowing them to be turned on or off remotely. This feature, combined with the ESP module's ability to control sockets even when their physical switches are off, highlights the system's robustness and flexibility. To maximize the smart socket's potential, further emphasis should be placed on expanding its scalability and enhancing user accessibility through advanced smartphone applications. This comprehensive integration of sensors and ESP modules not only augments the smart socket's functionality but also underscores the importance of innovation in creating energy-efficient and user-friendly smart home solutions.

In the smart socket system, MQTT (Message Queuing Telemetry Transport) plays a pivotal role in facilitating communication between devices, leveraging its lightweight and efficient design to operate effectively in resource-constrained environments such as those involving smart home devices. The protocol's publish-subscribe architecture simplifies the communication process, allowing the smart sockets to not only send but also receive messages from a central control unit like the NodeMCU, which orchestrates the system's operations. This design ensures that the smart socket can efficiently manage its power usage and maintain reliable connections even when network conditions are less than ideal, further enhancing the system's overall efficiency and reliability. Given these capabilities, MQTT is particularly well-suited for smart socket systems, ensuring seamless and robust communication that is crucial for real-time monitoring and control of home appliances. This underscores the necessity for adopting MQTT in environments where efficient and reliable communication is paramount, especially as smart home technologies continue to evolve and demand more sophisticated connectivity solutions.

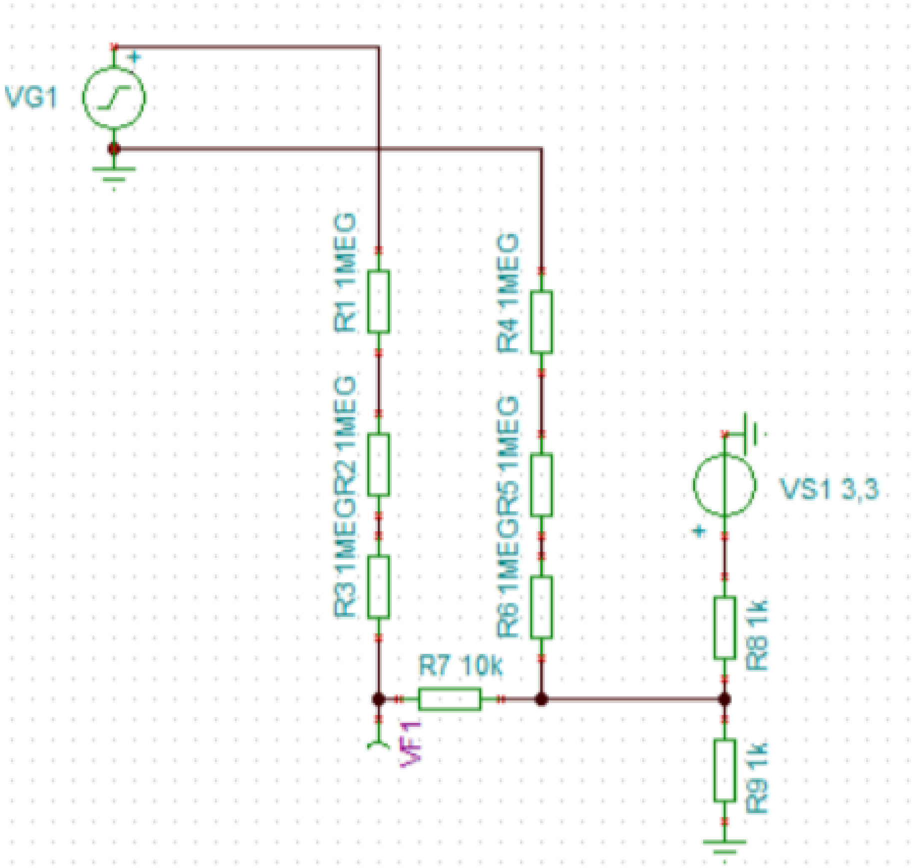

Fig. 1 Power circuit for voltage measurements

The smart socket's architecture was designed to balance compactness, cost-efficiency, and functionality. It integrates several key components: an ESP32C3 microcontroller for control and communication, an ACS712 sensor for current measurement, and voltage divider circuits for safe voltage monitoring. The system communicates with a centralized server using the MQTT protocol and presents real-time data to the user through a Node-RED dashboard. The final prototype integrates all hardware components into a custom-designed enclosure. The enclosure was produced using 3D printing to accommodate the PCB and other electronics. This design ensures the device is robust and suitable for household use.

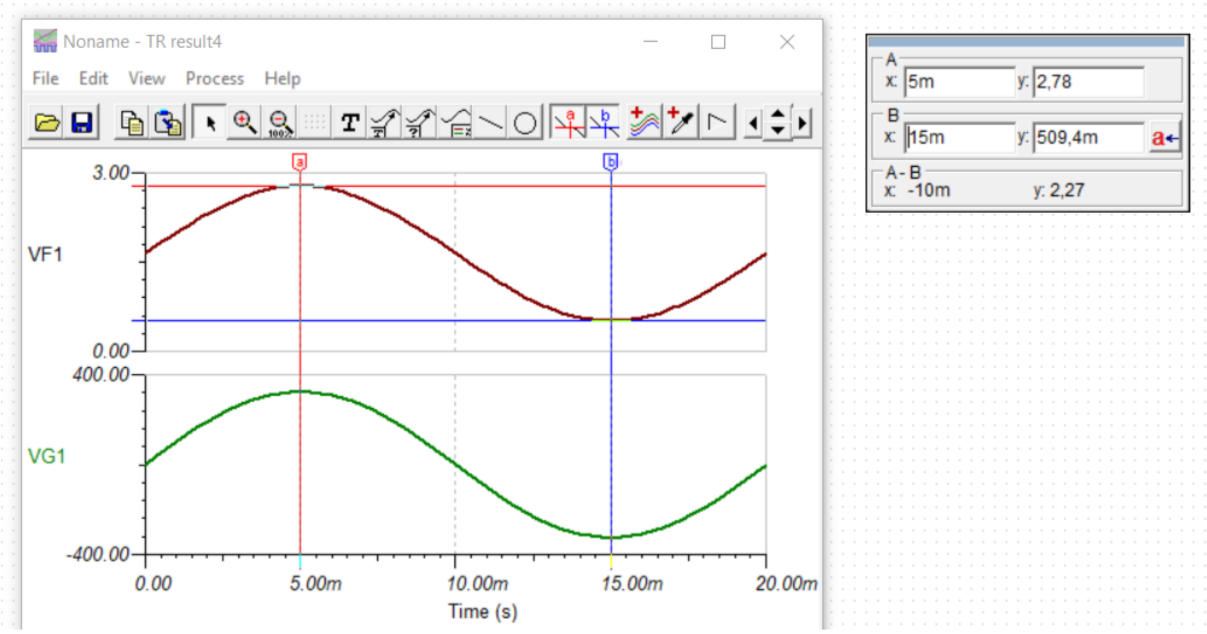

Fig. 2 Simulation of the power circuit for voltage measurements performance

Fig. 3 Final PCB of the device

III. Conclusion

The smart socket demonstrated reliable performance in monitoring and controlling energy consumption. The results validate the smart socket's potential as an effective tool for residential energy management. By combining real-time monitoring, remote control, and user-friendly interfaces, the system addresses key limitations of traditional energy management solutions. However, challenges such as integrating the system with existing home automation platforms and optimizing sensor performance under extreme conditions were identified during testing. Future work could focus on expanding the system's capabilities, such as adding machine learning algorithms for predictive energy analysis or integrating with renewable energy sources to further enhance sustainability. This study presents a smart socket system designed to empower users with real-time energy monitoring and control capabilities. By leveraging IoT technologies and cost-effective components, the system provides a scalable and user-friendly solution for optimizing household energy consumption. The successful implementation and testing of the smart socket underscore its potential to contribute to sustainable energy practices. Future research should explore expanding the system's functionality and integrating it with broader smart home ecosystems.

References

[1] J. Gubbi, R. Buyya, S. Marusic, and M. Palaniswami, "Internet of Things (IoT): A Vision, Architectural Elements, and Future Directions," *Future Generation Computer Systems*, vol. 29, no. 7, pp. 1645-1660, 2013.

[2] International Energy Agency (IEA), *Energy Efficiency 2021*, IEA, 2021.

[3] Espressif Systems, *ESP32 Technical Reference Manual*, 2020.

[4] L. Atzori, A. Iera, and G. Morabito, "The Internet of Things: A Survey," *Computer Networks*, vol. 54, no. 15, pp. 2787-2805, 2010.

[5] A. Kumar and R. Singh, "IoT-Based Smart Energy Monitoring Systems: A Review," *IEEE Sensors Journal*, vol. 21, no. 2, pp. 1234-1242, 2021.

Remote Controlled Bait Boat

Miroslav Jančo, Michal Hodoň, Lukáš Čechovič

***Abstract*—** In this paper, we focused on the design and implementation of a remote controlled bait boat for fishing, which is capable of efficiently distributing bait or feed on the water surface. For this purpose, we utilized the ESP32 microcontroller, along with the ESP-NOW communication protocol, which enables wireless control of the boat. Additional technologies include the use of 3D printing to manufacture components of the boat and the development of software to manage its operations. During the development, we faced various challenges, including optimizing the boat's design and ensuring stable communication between the boat and the control device. We overcame these issues through repeated testing and enhancements in the hardware design and software functionality. The result is a functional prototype of the bait boat, which can precisely and reliably place baits in various fishing environments, thus enhancing the efficiency of fishing and minimizing disruption to the aquatic ecosystem.

***Keywords*—** ESP32, ESP-NOW, Remote Control, Bait Boat.

I. Introduction

The advancement of technology has significantly transformed various industries, including recreational fishing, where the integration of automation and wireless communication has opened new avenues for enhancing fishing efficiency and sustainability. This research paper presents the design and implementation of a remote-controlled bait boat, specifically engineered to facilitate the precise distribution of bait on the water surface. Central to this development is the ESP32 microcontroller, a powerful and versatile device that not only manages the boat's operations but also supports the innovative ESP-NOW communication protocol, which allows for seamless and reliable wireless control over considerable distances. This technology is particularly beneficial for fishing, as it enables anglers to deploy bait accurately without disturbing the aquatic environment. Furthermore, the project employs 3D printing techniques to fabricate custom components, thereby streamlining the manufacturing process and allowing for rapid prototyping of the bait boat's design. Throughout the development phase, we encountered various challenges such as optimizing the vessel's design for stability and ensuring uninterrupted communication between the control device and the boat itself. Through iterative testing and enhancements in both hardware and software, we successfully addressed these issues, culminating in a functional prototype capable of operating effectively in diverse fishing scenarios. Ultimately, this research not only contributes to the field of fishing technology but also emphasizes the importance of minimizing ecological impact while maximizing angling success, thus offering a novel solution that aligns with contemporary conservation efforts.

II. Integration

The ESP32 microcontroller plays a crucial role in the operation of bait boats by integrating various functionalities essential for autonomous navigation and control. At the core of its capabilities, the ESP32 MCU facilitates the bait boat's ability to autonomously navigate to predetermined locations, thereby serving as a buoy for divers [1]. This autonomous navigation is made possible through the microcontroller's ability to process and execute complex algorithms that interpret environmental data and adjust the boat's course accordingly. Additionally, the ESP32 enables users to remotely input GPS coordinates via a mobile application, leveraging GPRS connectivity to communicate these coordinates to the bait boat

Miroslav Jančo, University of Zilina, Zilina, Slovakia (e-mail: janco@stud.uniza.sk)
Michal Hodoň, University of Zilina, Zilina, Slovakia (e-mail: michal.hodon@fri.uniza.sk)
Lukáš Čechovič, University of Zilina, Zilina, Slovakia (e-mail: lukas.cechovic@fri.uniza.sk)

[1]. This feature not only enhances the convenience of operating the bait boat but also expands its functionality by allowing precise and remote navigation to locations that may be difficult to reach manually. Furthermore, the ESP32 controls the circuit implemented within the bait boat, ensuring seamless integration of its electrical components and enabling efficient power management and operation [1]. By acting as the central processing unit, the ESP32 coordinates the communication between sensors, motors, and other electronic modules, ensuring that the boat operates smoothly and effectively. These interconnected functionalities underscore the ESP32 microcontroller's pivotal role in enhancing the operational efficiency and versatility of bait boats. To fully leverage these capabilities, ongoing maintenance and software updates are essential to adapt to evolving technological standards and environmental conditions, ensuring continued reliability and performance.

The incorporation of the ESP-NOW communication protocol within the control system of the bait boat significantly enhances its operational efficiency and responsiveness. As ESP-NOW is designed specifically for ESP8266 and ESP32 microcontrollers, it provides an optimal fit for the ESP32 MCU utilized in the bait boat control system [2]. By operating in a peer-to-peer communication mode, ESP-NOW allows the bait boat to communicate directly with other devices, such as GPS modules and control systems, without the need for a traditional Wi-Fi connection or access point [2]. This direct communication is crucial for sensor networks and automation applications, making ESP-NOW ideal for the bait boat's requirements where rapid and efficient data transmission is essential [2]. Furthermore, the protocol's low-latency data transmission capabilities ensure that commands from the mobile application are executed in real-time, allowing for precise navigation and control of the bait boat [2]. Additionally, the absence of a complex network infrastructure requirement enhances the bait boat’s ability to function effectively in diverse environments, including remote or offshore locations [2]. Adopting the ESP-NOW protocol in the bait boat system not only streamlines communication but also maximizes the ESP32's capabilities in wireless communications, thereby improving the overall reliability and performance of the autonomous navigation system [2].

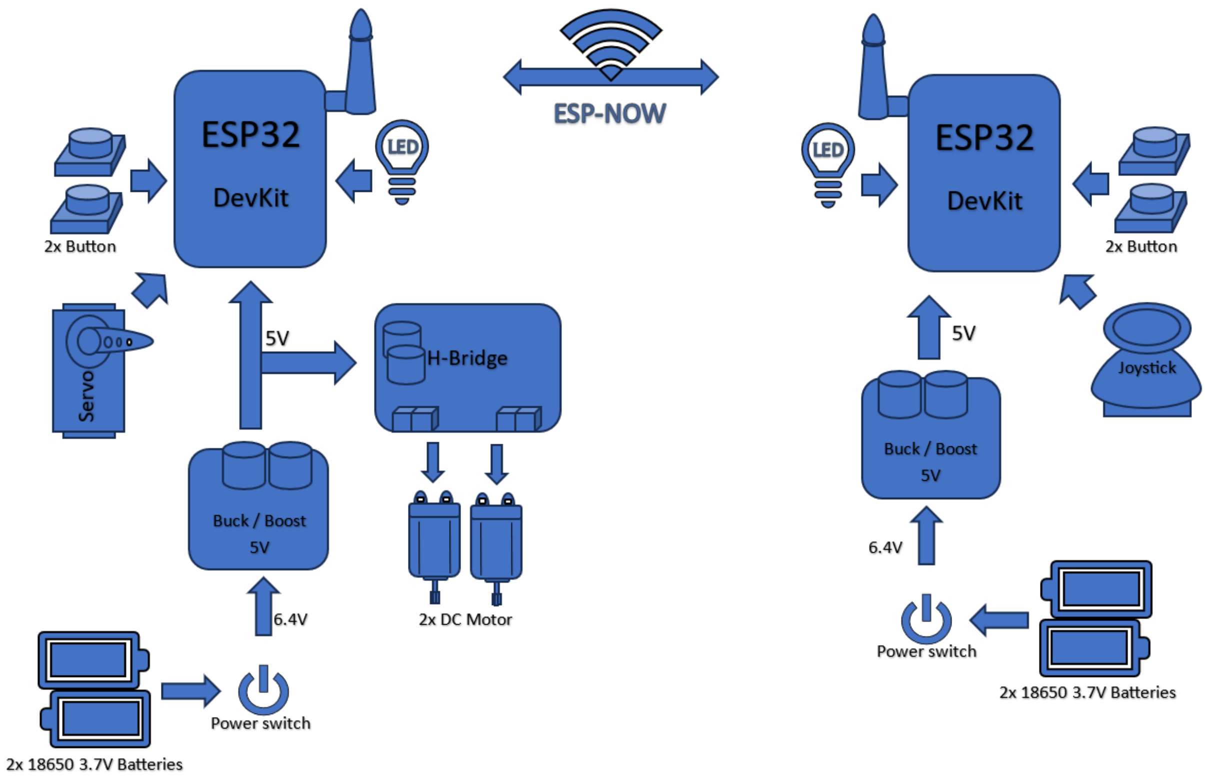

Fig. 1 System block schematic

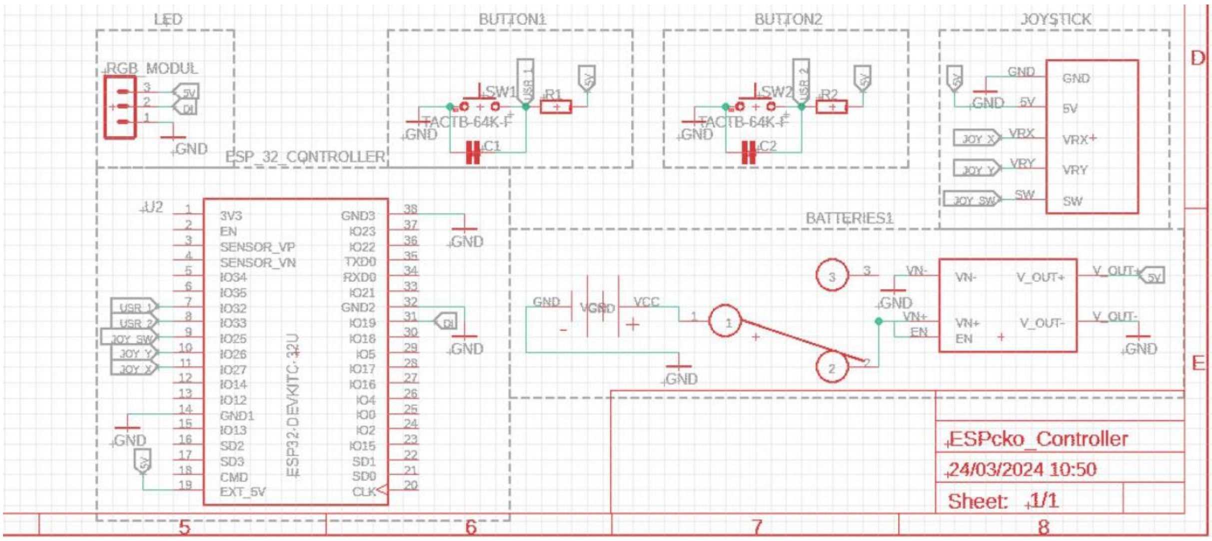

Fig. 2 Driver electric schematic

The integration of 3D printing technologies in the manufacturing of boat components has revolutionized traditional processes, offering enhanced flexibility and functionality. A notable application of 3D printing in this domain is the creation of water jet propulsion systems using PLA (polylactic acid) material, which not only contributes to the environmental sustainability of manufacturing practices due to its biodegradable nature but also allows for precise customization and rapid prototyping [3]. The thermoplastic properties of PLA enable it to be molded into complex shapes, which is essential in fabricating intricate components like hulls that require the integration of electrical systems for efficient propulsion [3]. This integration is evident in the construction of prototype boats, where the 3D-printed hulls are designed to seamlessly incorporate and secure these electrical components, enabling direct connectivity with the propulsion systems [3]. After the installation of these systems, a functionality check is conducted to ensure that the components operate as intended, thereby demonstrating the practical utility and effectiveness of 3D printing in real-world boat manufacturing scenarios [3].

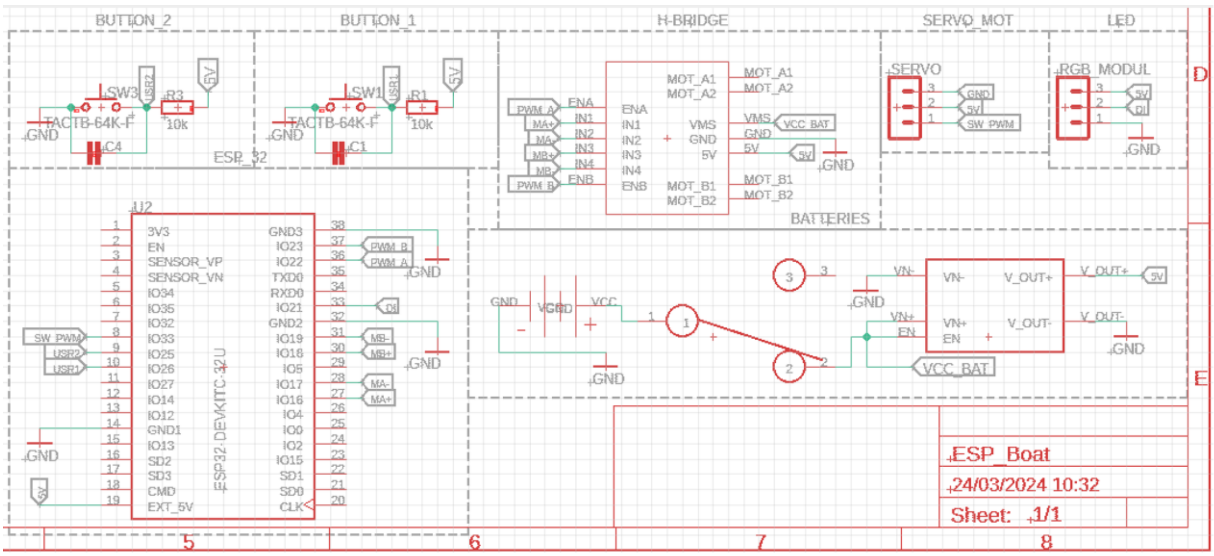

Fig. 3 Boat control board electric schematic

The use of 3D printing in such applications not only accelerates the manufacturing process but also enhances the adaptability of design, allowing for modifications and improvements tailored to specific performance requirements. These advancements underscore the potential of

3D printing to not only complement but also innovate traditional manufacturing methods, highlighting the need for further research and development to fully harness its capabilities in the boating industry.

III. Conclusion

The integration of the ESP32 microcontroller into the design and functionality of remote-controlled bait boats represents a significant advancement in autonomous marine technology, particularly in enhancing navigational precision and operational efficiency. The ability to autonomously navigate to predetermined GPS coordinates, as facilitated by the ESP32's sophisticated processing capabilities, not only streamlines the deployment of bait but also broadens the application scope of such vessels, particularly in recreational fishing and underwater exploration. This work demonstrates how advancements in microcontroller technology, combined with mobile application interfaces, can create systems that are both user-friendly and highly functional, allowing for real-time adjustments based on environmental data. However, despite these promising developments, there are notable limitations that warrant further investigation. For instance, the dependency on GPRS connectivity raises concerns about the reliability of communication in remote areas with poor signal coverage, highlighting a gap in the current implementation that could affect navigational accuracy and operational reliability. Additionally, while 3D printing offers remarkable benefits in terms of customization and rapid prototyping, the long-term durability and performance of 3D printed materials under various marine conditions need thorough evaluation to ensure that these components can withstand the rigors of aquatic environments. Future research should focus on enhancing the robustness of the communication systems, exploring alternative or supplementary technologies for navigation in challenging environments, and assessing the longevity of 3D printed materials in marine applications. By addressing these limitations, the findings from this study can be expanded upon, paving the way for more resilient and versatile autonomous vessels in the boating industry. The potential for innovations stemming from this research not only contributes to academic discourse but also has practical implications for the design and operation of marine technology, emphasizing the need for continuous exploration and development in this rapidly evolving field.

References

[1] [1] C. Albacete Fuentes, *Scale boat guidance through mobile application*, [Online]. Available: digibug.ugr.es/handle/10481/88000. [Accessed: Dec. 1, 2024].

[2] [2] *Practical guide to ESP32 communication protocols*, [Online]. Available: www.techrm.com. [Accessed: Dec. 1, 2024].

[3] [3] B. Kaushik, B. Kumar, B. Harathi, and A. Sai, *A4*, [Online]. Available: www.nriims.info/mechanical/PROJECT15-19/A4.pdf. [Accessed: Dec. 1, 2024].